6250–6268 *Nucleic Acids Research, 2019, Vol. 47, No. 12* *Published online 22 April 2019*
doi: 10.1093/nar/gkz279

The telomeric Cdc13–Stn1–Ten1 complex regulates RNA polymerase II transcription

Olga Calvo [1,*,†], Nathalie Grandin [2,†], Antonio Jordán-Pla [3], Esperanza Miñambres [1], Noelia González-Polo [1], José E. Pérez-Ortín [3] and Michel Charbonneau [2,*]

[1]Instituto de Biología Funcional y Genómica, CSIC-USAL, Salamanca, Spain, [2]GReD laboratory, CNRS UMR6293, INSERM U1103, Faculty of Medicine, University Clermont-Auvergne, 28 place Henri Dunant, BP 38, 63001 Clermont-Ferrand Cedex, France and [3]ERI Biotecmed, Facultad de Ciencias Biológicas, Universitat de València, C/Dr. Moliner 50, E46100 Burjassot, Spain

Received January 09, 2019; Revised March 18, 2019; Editorial Decision April 06, 2019; Accepted April 08, 2019

ABSTRACT

Specialized telomeric proteins have an essential role in maintaining genome stability through chromosome end protection and telomere length regulation. In the yeast *Saccharomyces cerevisiae*, the evolutionary conserved CST complex, composed of the Cdc13, Stn1 and Ten1 proteins, largely contributes to these functions. Here, we report genetic interactions between *TEN1* and several genes coding for transcription regulators. Molecular assays confirmed this novel function of Ten1 and further established that it regulates the occupancies of RNA polymerase II and the Spt5 elongation factor within transcribed genes. Since Ten1, but also Cdc13 and Stn1, were found to physically associate with Spt5, we propose that Spt5 represents the target of CST in transcription regulation. Moreover, CST physically associates with Hmo1, previously shown to mediate the architecture of S-phase transcribed genes. The fact that, genome-wide, the promoters of genes down-regulated in the *ten1-31* mutant are prefentially bound by Hmo1, leads us to propose a potential role for CST in synchronizing transcription with replication fork progression following head-on collisions.

INTRODUCTION

Telomeres consist of an elaborate, high-order assembly of specific TG-rich repetitive DNA sequences and proteins that cooperatively provide protection against chromosome degradation. A number of telomeric proteins have been identified and, together, they act to 'cap' the telomere and 'hide' it from cellular DNA repair, including recombination (1). If left unprotected, telomeres are recognized by the cell as DNA double-strand breaks, leading to recombination, chromosome fusions and broken and rearranged chromosomes. Telomeric DNA is replicated by a specialized reverse transcriptase enzyme, telomerase. In addition, telomeres recruit specialized proteins to prevent telomere degradation and regulate telomere length, including the recruitment of telomerase at telomere ends. In vertebrates, telomere protection is provided mainly by shelterin, a complex of six telomeric proteins, TRF1, TRF2, POT1, TIN2, TPP1 and RAP1 (2,3). A similar complex exists in the fission yeast *Schizosaccharomyces pombe* (4), while in the budding yeast *Saccharomyces cerevisiae* a somewhat simpler telomeric complex, called CST, consisting mainly of the Cdc13, Stn1 and Ten1 proteins is present (5–7). Orthologs of *S. cerevisiae* CST have been found in humans and mouse, as well as in *S. pombe* and the plant *Arabidopsis thaliana* (8–10). Recently, hCST was found to associate with shieldin at damaged telomeres to regulate, in association with Polα, the fill-in of the resected overhangs and facilitate DNA repair (11). In yeast, Stn1 has also been implicated in the fill-in of the strand previously elongated by telomerase (12,13). Based on the hypersensitivity of mutants of CST to DNA damaging agents and its presence at sites other than the telomeres, hCST has emerged as an important potential player in counteracting replication stress genome-wide (9,14,15).

Transcription by RNA polymerase II (RNA Pol II) is achieved through different steps (preinitiation, initiation, elongation and termination), and is highly regulated by a huge number of factors, including general transcription factors, cofactors, elongation and termination factors. Over

*To whom correspondence should be addressed. Tel: +33 473 407 752; Email: michel.charbonneau@uca.fr
Correspondence may also be addressed to Olga Calvo. Tel: +34 923 294 904; Email: ocalvo@usal.es
Present address: José E. Pérez-Ortín, SciLifeLab, Department of Microbiology, Tumor, and Cell Biology, Karolinska Institute, Tomtebodavägen 23, SE-171 21, Stockholm, Sweden.
†The authors wish it to be known that, in their opinion, the first two authors should be regarded as Joint First Authors.

the last decade, transcription elongation has been shown to also be a crucial and strictly regulated step of transcription (16). Among RNA Pol II regulators, Spt5/NusG is the only family of transcription factors that has been evolutionary conserved, from Bacteria to Eukarya. In Eukarya and Archea, Spt5 forms a heterodimeric complex with Spt4 (17). Spt4/5 associates with genes from downstream of the transcription start site to the termination sites, with a distribution pattern similar to that of RNA Pol II (18). Accordingly, Spt4/5 associates with RNA Pol II in a transcription-dependent manner (19). In addition, Spt4/5 links the activities of the transcription elongation complex to pre-mRNA processing and chromatin remodeling (20,21). Although there has been until now no functional evidence for a role of Spt5 in connecting transcription with DNA replication, it is nevertheless noticeable that the DNA polymerases subunits Pol1 and Pol2 were identified as Spt5-associated proteins (22).

Phosphorylation of the C-terminal domain (CTD) of RNA Pol II largest subunit, Rpb1, which consits of an evolutionary conserved repeated heptapeptide motif (Tyr1-Ser2-Pro3-Thr4-Ser5-Pro6-Ser7), regulates RNA Pol II transcription at several levels (23,24). CTD-Ser2 and -Ser5 phosphorylation (Ser2P and Ser5P) appear to be the most frequent modifications (25,26). Ser2P is the mark of the elongating polymerase, while Ser5P marks the initiation step. The large number of possible CTD modifications generate a 'CTD code' that coordinates the recruitment of numerous factors essential for transcriptional efficiency, RNA processing and connects transcription with other nuclear processes (27–29). In *S. cerevisiae*, four cyclin-dependent kinases, Srb10, Kin28, Ctk1, and Bur1 (30,31) and four phosphatases, Rtr1, Ssu72, Glc7 and Fcp1 (32,33) determine CTD phosphorylation along the transcription cycle. During early elongation, Bur1 phosphorylates CTD-Ser2 and Spt5 nearby the promoters (21,34), while Ctk1 phosphorylates Ser2 later during elongation, its activity being required for termination and 3′-end processing (35). Fcp1 dephosphorylates Ser2P and its activity opposes that of Ctk1 to ensure proper levels of Ser2P during elongation and RNA Pol II recycling (36).

In this study, we have uncovered specific genetic interactions between *TEN1* and several genes coding for transcriptional regulators, such as *BUR1*, *FCP1*, *SPT5, SPT4*, *CDC73* and *RPB1*. We demonstrate that Ten1 physically interacts with Spt5 and regulates its association with chromatin during active transcription. Stn1 and Cdc13 were also found to exhibit physical interactions with Spt5. Moreover, genome-wide data show that the *ten1-31* mutation altered RNA Pol II gene occupancy, as demonstrated by ChIP-qPCR and ChIP-seq data. Additionally, we found that Ten1 physically interacts with the high-mobility group box (HMGB) protein Hmo1, previously implicated in transcription regulation, as well as in solving difficult topological contexts when transcription has to face incoming replication forks (37). Based on our data, we propose a working model in which CST, traveling with the replication fork, could stimulate the restart of the transcription machinery following head-on collisions with the progressing replication forks.

MATERIALS AND METHODS

Yeast strains, plasmids and media

Yeast culturing has been described previously (6). All *S. cerevisiae* strains used in this study were in the BF264-15Daub (*ade1 his2 leu2-3,112 trp1-1a ura3Dns*) genetic background used in the Charbonneau laboratory (6). All strains were made isogenic by back crossing at least five times against our genetic background. The *bur1-80-KanMX4*, *cak1-23-KanMX4*, *spt5-194-KanMX4*, *rpo21-1-KanMX4*, *fcp1-1-KanMX4*, *ssu72-2-KanMX4*, *kin28-ts-KanMX4*, *spt4*::*KanMX4*, *cdc73*::*KanMX4*, *srb10*::*KanMX4*, *pho85*::*KanMX4*, *ctk1*::*KanMX4*, *rtr1*::*KanMX4*, *thp2*::*KanMX4*, *mft1*::*KanMX4*, *rnh1*::*KanMX4*, *rnh201*::*KanMX4*, *mrc1*::*KanMX4* and *ctf18*::*KanMX4* strains were purchased at Euroscarf (Frankfurt, Germany). The *top1*::*LEU2* and *top2-1* strains were kindly provided by Rolf Sternglanz.

The *ten1-16* (F154I) and *ten1-31* (E58K, L76P, E91V and V115A) mutants have been previously described (7). The *ten1-33* harbours the K40E, I44M, K55E and L76P mutations. All three *ten1* mutants are temperature-sensitive at different levels, exhibiting more or less growth impairement at 36°C. None of these three mutants exhibit a tight arrest, and all of them exhibit morphological defects at all temperatures comprised between 24 and 36°C, at various levels depending on the allele concerned. In all *ten1* mutants, the ORF was under the control of its natural promoter, expressed from a centromeric plasmid of the YCplac series (38) in strains in which *TEN1* had been completely deleted either by *LEU2* or *KanMX4* (7). It is important to note that *ten1-16*, *ten1-31* and *ten1-33* were totally inviable when present at single copy following expression from an integrative YIplac vector, as reported before (7), and had, therefore, to be expressed from a YCplac vector (38). Such CEN vectors are known to express genes under their control at 2–4 copies (39). This was not the case for *ten1-3*, *ten1-6* and *ten1-13*, which are not temperature-sensitive mutants and were isolated on the basis of conferring elongated telomeres and can be expressed under viable conditions from an integrative vector (7).

Plasmids expressing the *ten1-31-STN1*, *ten1-31-CDC13* or *TEN1-STN1* in-frame fusion genes were constructed by cloning in a centromeric plasmid the entire ORF of the first part of the hybrid gene plus upstream promoter sequences, in front of the ORF (which included its natural stop codon) of the second part of the hybrid gene. The codon for the first amino acid of the second protein in the hybrid construct was directly following the codon for the last amino acid of the first protein, in reading frame with it.

For immunoprecipitation and mass spectrometry experiments, strains harbouring either endogenous copy of Ten1-Myc_{13} or Stn1-Myc_{13} (40) or of Cdc13-Myc_{13} (41) were used. The construct for tagging endogenous *HMO1* with HA_2 at its C-terminus was made by using Polymerase Chain Reaction (PCR) to adapt the relevant restriction sites to the sequence of the gene and details of the construct can be available upon request.

The viability of cells previously grown in liquid was determined by performing and analysing the so-called 'drop

tests' or 'spot assays'. To do this, cells from exponential growth cultures were counted with a hematocytometer and the cultures were then serially diluted by 1/5th or 1/10th and spotted onto YEPD (or selective medium) plates and incubated at the desired temperatures for 2–3 days before being photographed. In some cases, cells were just restreaked onto YEPD plates and growth evaluated by visualizing the numbers and sizes of the growing colonies.

Genetic screen to find extragenic mutations enhancing the *ten1* phenotype

For strain mutagenesis, *ten1* mutant strains were grown overnight, almost to saturation, in liquid YEPD medium at 24°C, before being diluted 1/5000th to 1/7500th in 1 ml H_2O, from which 200 μl were plated out onto solid YEPD plates, which were then exposed to UV light (254 nm wave length) at a distance of 10–15 cm for 6–10 s. Plates of UV-mutagenized yeast strains were then incubated at 24°C for ∼50 h before being replicated on YEPD plates at 36°C. After 1.5–2.5 days, the 24°C and 36°C replicas were compared between them; colonies failing to grow well at 36°C were selected and their 24°C counterpart repatched at 24°C before being re-tested for growth at 36°C.

Co-immunoprecipitation (co-IP) and western blot analysis

A strain expressing Ten1-Myc_{13} or Cdc13-Myc_{13} or Xrs2-Myc_{13} strain for a negative control, were grown in 200 ml of YEPD to an OD 600 of 1.5, harvested, washed with water, and suspended in 2.5 ml of lysis buffer (20 mM HEPES pH 7.6, 200 mM potassium acetate, 1 mM EDTA pH 8.0, glycerol 10%) containing protease and phosphatase inhibitors. The cell suspension was flash frozen in liquid nitrogen, and then ground in a chilled mortar to a fine powder. Afterwards, the cell lysate was thawed and centrifuged at 13.200 rpm for 20 min. The supernatant was collected and total protein concentration was estimated measuring absorbance at 280 nm in a nanodrop. Prior to immunoprecipitation, the extracts were precleared by incubation with either protein G agarose (Santa Cruz) or protein A sepharose (GE healthcare) for 1 h to eliminate as much as possible unspecific binding. They were then centrifugated and the supernatants used for either anti-Myc or anti-Spt5 immunoprecipitations. For that, the volume of each cell extract containing 20 μg of protein was incubated with 1 μl of anti-Myc (Roche) or 2.5 μl of anti-Spt5 (Santa Cruz) for 1 h at 4°C, and afterwards 20 μl of protein A sepharose or protein G agarose slurry, respectively, were added and the incubation extended to overnight at 4°C. The IPs were extensively washed with lysis buffer and beads were suspended in SDS-PAGE sample buffer. Thereafter they were incubated at 65°C for 20 min and supernatants were loaded onto a SDS-PAGE gel and analysed by western blot with the corresponding antibodies. For Ten1-Myc_{13}/Hmo1-HA_2 co-IP assays, we proceeded as above. In that case, 20 μg of whole cell extracts from Ten1-Myc_{13}, Hmo1-HA_2 and Ten1-Myc_{13} Hmo1-HA_2 strains were IPed with 2 μl of anti-Myc, and then assayed by western blot using anti-HA and anti-Myc antibodies.

Measurements of telomere length and detection of telomeric single-stranded DNA (ssDNA)

For detection of telomeric ssDNA on dot blots, genomic DNA was digested with *Xho*I, denatured (denatured blot) or not (native blot) and then loaded on a BioRad dot blot apparatus, as previously described (7). The membrane was then hybridised to a 270 bp TG_{1-3} ^{32}P-labelled probe representing *S. cerevisiae* telomeric sequences. Results were analysed with a Typhoon phosphorimager (GE Healthcare) and quantified using ImageQuant TL.

Two-hybrid experiments

Experiments of protein-protein interactions using the two-hybrid system were performed as described previously (6,42,43). Genes of interest were cloned in-frame with the *GAL4* activation domain (nucleotides 764–885) in pACT2 or in-frame with the *GAL4* DNA-binding domain (nucleotides 1–147) in pAS2. Both types of constructs were transformed into the Y190 strains, which were then tested for β-galactosidase activity, toghether with the appropriate controls, as described previously (43) using X-gal (5-bromo-4-chloro-3-indolyl-p-D-galactopyranoside, from Sigma).

RNA isolation and RT-PCR

Total RNA was extracted as described (44) and RT-PCR was performed using the iScript RT reagent kit (Bio-Rad), following the manufacturer's instructions. PCR reactions were performed in triplicate with at least three independent cDNA samples.

RNA-seq

Library preparation, sequencing and quality control. Yeast total RNA was extracted from *ten1-31* mutant and wild-type (*wt*) cells after shifting to restrictive temperature, 34°C, for 2 h. RNA from three biological replicates of the experiment was prepared independently for each condition (total of six samples) and subjected to rRNA depletion. The rRNA depleted fraction was then used to construct libraries that were sequenced in a HiSeq system (Ilumina) to an output of 120 (1 × 50 nt) million strand-specific reads. Raw reads were analysed with FastQC to make sure each sequenced sample met the adequate quality standards.

Adapter clipping, quality trimming and filtering. Trimmomatic (45) was used to clip, filter and remove certain portions of reads or even entire reads. The Illuminaclip function was used to remove Illumina adapters. The SLIDINGWINDOW function was applied to filter out reads shorter than 20 bases and the MINLEN function was used to discard reads with an average quality of <28. A second round of inspection with FastQC was carried out after the filtering steps to ensure that the filters were applied properly.

Genome alignment and expression matrix generation. Filtered reads were mapped to the yeast genome with TopHat2 (46), using the R64 (sacCer3) genome as reference. 94.7% of total reads were successfully aligned to the reference genome. A table with information about *per sample* total

number of reads, trimmed and quality-filtered reads and overall alignment rates is provided as Supplementary Table S1. BAM alignment files were visually inspected with the genome browser IGV (www.broadinstitute.org/igv/). Normalised coverage tracks for genome browser visualization were generated with the functions bamCoverage and bamCompare from the deepTools2 suite (47). Coverage tracks from individual samples are expressed as reads per kilobase per million mapped reads (RPKM), whereas comparison tracks are expressed as the $\log_2$ of the number of reads ratio. Raw read counts were extracted with the featureCounts tool from the R package Rsubread (48), using the yeast genome annotation as a reference.

Similarity of biological replicates. The similarity of biological replicates was assessed with correlation analysis after $\log_2$ transformation of the raw read expression matrix. The function heatpairs from the R package LSD (https://CRAN.R-project.org/package=LSD) was used to generate a matrix of pairwise correlation scatterplots. Spearman correlation coefficients are reported by default for each comparison (see Results section). The raw expression matrix was used as input for differential expression analysis.

Differential expression analysis and GSEA. The list of differentially expressed genes between samples was obtained by using DESeq2 after applying a 0.3 non-differential contig count quantile threshold and a 0.05 *P*-value threshold for the FDR control test. Changes in expression between *ten1-31* and wt samples are expressed as $\log_2$ Fold Change (mutant/wt). The list of genes with $\log_2$ FC values as calculated by DESeq2 was ordered from highest to lowest and used as input to test for GO category enrichment, as implemented in GOrilla (49).

Chromatin immunoprecipitation (ChIP)

Chromatin purification, immunoprecipitation, quantitative real-time PCR (qPCR) amplification and data analysis were performed as described (44,50,51). Briefly, cells were grown overnight to saturation at 25°C, then diluted to an OD_{600} of ∼0.2, and let them grow at 34 °C for ∼5 h until they reached an OD_{600} of 0.5–0.6. Immunoprecipitated and purified chromatin was subjected to quantitative real-time PCR using the CFX96 Detection System (Bio-Rad Laboratories, Inc.) and SYBR® Premix Ex Taq™ (Takara Bio), following the manufacturer's instructions. Real-time PCR reactions were performed in duplicate from at least three independent ChIPs. Quantitative analysis was performed with the CFX96 Manager Software (version 3.1, Bio-Rad). The values obtained for the IPed PCR products were compared to those of the total input, and the ratio of the values from each PCR product from transcribed genes to a non-transcribed region of chromosome VII was calculated. Numbers on the y-axis of graphs are detailed in the corresponding figure legend.

ChIP-seq

Library preparation, sequencing and quality control. For ChIP-seq experiments, anti-mouse or anti-rat IgG dynabeads (Invitrogen) were used to immunoprecipitate Rpb1 or Rpb1-Ser2P, together with 8WG16 and 3E10 antibodies, respectively. Each experiment was carried out in biological duplicates for a total of 12 samples. Library DNA was prepared from immunoprecipitated DNA and its corresponding input DNA following the manufacturer's instructions, and was sequenced in a Illumina HiSeq 2500 system to an output of 313 (1 × 50) million reads. The quality metrics of the fastq sequencing datasets were obtained with FastQC and visually inspected.

Filtering, trimming and adapter clipping. These steps were carried out essentially as described for RNA-seq.

Genome alignment and genome browser visualization. High quality reads were mapped to the yeast genome with Bowtie2 (52), using the R64 (sacCer3) genome as reference. A table with alignment statistics is provided as Supplementary Table S2. BAM alignment files were visually inspected with the genome browser IGV. Normalised coverage tracks for genome browser visualization were generated with the functions bamCoverage and bamCompare from the deepTools2 suite (47). Coverage tracks from individual samples are expressed as reads per kilobase per million mapped reads (RPKM), whereas comparison tracks are expressed as the $\log_2$ of the number of reads ratio.

Reproducibility of the replicates and merging of datasets. A matrix of read coverages for the entire genome was generated with all alignment files with the function multiBamSummary from deepTools2. Briefly, the function takes the genome annotation and splits it in 10 kb bins. For each bin, the number of reads found in each bam dataset is counted. A correlation matrix heatmap plot was generated with the plotCorrelation function of the same package. Correlation values are calculated with the Spearman method as default (see below in Results section). Based on the high correlation values of the biological replicates, the two datasets from each sample were merged into one for average metagene representations around genomic regions with SamTools (53).

Metagene analysis. Normalised average density plots around genomic features were calculated with the ngs.plot software (54). The ChIP-seq mode and the statistical robustness parameter, which filters out 0.5% of genes with the most extreme occupancy values, were applied to all calculations.

ChIP-exo of Hmo1. Hmo1 ChIP-exo datasets (55) were downloaded from the Sequence read archive (SRA) repository, with accession number SRP041518. Raw fastq files were processed following a pipeline similar to the one described above for our ChIP-seq datasets.

Mass spectrometry analysis

Anti-Myc immunoprecipitates from a Ten1-Myc_{13} (or Stn1-Myc_{13}) strain or control isogenic untagged strain were loaded in a SDS-PAGE acrylamide concentrator gel and run for a very short time, after which, the sample-containing bands were cut out and digested with trypsin using and automatic digestion robot (Bruker Proteineer) under reducing

(DTT) conditions. Carbamidomethylation of the samples was then performed using iodoacetamide. After digestion, samples were dried and dissolved in a final volume of 15 μl. A total volume of 5 μl of each sample was analysed by liquid chromatography (short gradient, 100 min) coupled to a QTOF mass spectrometer (5600 Triple-TOF) along which the peptides were separated as a function of their hydrophobicity (using a C-18 reversed phase column). The eluted peptides were then fragmented on the 5600 Triple-TOF mass spectrometer, thereby obtaining a high number of MS and MSMS spectra of the precursors (peptides) present in the sample. Raw data were exported, processed and used to launch a search against the Uniprot *S. cerevisiae* database using the MASCOT search engine. Peptide identifications with Mascot scores equal or >20 were exported and used to establish the statistical significance of the identifications. False discovery rates (FDR) were applied at different levels: spectrum, peptide and protein, among which the protein level was considered for analysis. As generally accepted, a FDR value was considered to be significant when smaller than—or equal to—1%.

RESULTS

TEN1 genetically interacts with *BUR1* and *CAK1*

In contrast with *S. cerevisiae* Cdc13 and Stn1 that have been attributed major specific functions in telomere protection and length regulation, Ten1, also implicated in these pathways, has no known specific function besides being interacting with Stn1. To identify the functions of Ten1, we used three different *ten1* temperature-sensitive mutants in genetic screens aiming at identifying mutants that aggravated their growth defects at 36°C. Following screening of ∼ 40 000 colonies of UV-mutagenized *ten1* strains, only one, the *ten1-33* mut. #27 double mutant, satisfied our genetic criteria (see Materials and Methods). Following transformation of this double mutant with a genomic DNA library, a clone that suppressed the aggravated growth arrest at 36°C was isolated and the rescuing activity shown to be at the *SGV1*/*BUR1* locus (Figure 1A; see also Supplementary results). Sequencing the *BUR1* genomic locus of the *ten1-33 bur1-27* double mutant identified a single point mutation, P281L. This mutant allele of *BUR1* has been named *bur1-27*. The *bur1-27* single mutant was found to be temperature-sensitive at 36°C (Figure 1A). *CAK1* was also isolated in the same complementation experiment (Figure 1A), but only as an extragenic suppressor (see Supplementary results), and this is in agreement with the earlier finding that *CAK1* is a high-copy suppressor of a *bur1* mutation (56). However, *cak1-23* also exhibited synthetic growth defects with *ten1-31* (Figure 1B; see also Supplementary results), like *bur1-27* and *bur1-80* did (57,58).

Two additional temperature-sensitive *ten1* mutants, *ten1-16* and *ten1-100*, as well as two non temperature-sensitive *ten1* mutants, *ten1-3* and *ten1-6*, harbouring elongated telomeres (7), also exhibit synthetic growth defects with *bur1-80* (Supplementary Figure S1A). Importantly, overexpression of *TEN1* rescued *bur1-80* (Supplementary Figure S1B) and the observed synthetic lethality between the *ten1* and *bur1* mutations was not due to altered *TEN1* transcription (Supplementary results and Supplementary Figure S1C).

Cdc13 and Stn1 cooperate with Ten1 in transcription functions

Cdc13, Stn1 and Ten1 physically interact (6,7) to form the CST complex and there is evidence suggesting that Cdc13 and Stn1 perform overlapping but distinct functions. Given the genetic interactions between *TEN1* and *BUR1* and *CAK1*, we tested whether this was also the case between *BUR1* or *CAK1* and *STN1* and *CDC13*, the other two members of the CST complex. No obvious genetic interactions were observed between *cdc13-1* and *bur1-80* or *cak1-23,* nor between *stn1-13* and *bur1-80* or *cak1-23* (Figure 1C). In addition, *stn1-101* and *stn1-138*, two additional temperature-sensitive mutants of *STN1* (7,59) did not exhibit obvious synthetic growth defects with *bur1-80* (Supplementary Figure S1D). However, *stn1-154*, another temperature-sensitive mutant of *STN1* with a more severe phenotype than *stn1-101* and *stn1-138*, (7,59), did exhibit clear synthetic lethality with *bur1-80* (Figure 1D).

We next looked for further evidence for the implication of the whole CST complex in transcription. To this end we used fusion (hybrid) proteins, a method already applied with success in studies on Cdc13 and Stn1 (60,61). All hybrid genes were expressed from a centromeric plasmid under the control of the *TEN1* natural promoter. First, after expressing in a *ten1-31 bur1-80* mutant a Ten1-31-Stn1 fusion protein, we observed that the synthetic growth defects between *bur1-80* and *ten1-31* were totally suppressed (Figure 1E). A Ten1-31-Cdc13 fusion construct could also rescue the synthetic defect between *bur1-80* and *ten1-31* (Figure 1E). Most interestingly, expression of a *TEN1-STN1* hybrid gene allowed *ten1-31 bur1-80* mutant cells to grow even better than those expressing the *ten1-31-STN1/CDC13* fusions or *TEN1* alone, an effect seen at 34°C (Figure 1E). These experiments indicate that providing a permanent association between either Stn1 or Cdc13 and Ten1-31 (by means of expressing hybrid proteins) can eliminate the deleterious effects of the Ten1-31 mutant protein. In addition, providing a permanent association between wild-type Ten1 and Stn1 rescues *bur1-80* temperature sensitivity, a situation that is distinct from the synthetic lethality between *ten1-31* and *bur1-80*. From these experiments, we suggest that Stn1 and Cdc13 most probably cooperate with Ten1 in transcription functions, but that, based on genetics, Ten1 has a more direct and predominant role than those of Stn1 and Cdc13.

TEN1 genetically interacts with the RNA Pol II transcriptional machinery

In budding yeast, the main role of cyclin-dependent kinase (CDK)-activating kinase (CAK) is the activation of CDKs by phosphorylation (Supplementary results and Supplementary Figure S2A). Cdc28, Kin28, Bur1 and Ctk1, but not Srb10 and Pho85, are phosphorylated by Cak1. Interestingly, the *ten1-31* mutant exhibited genetic interactions with *kin28-ts*, but not with *srb10Δ* or *pho85Δ* (Supplementary Figure S2B, C and data not shown). On the other hand, *ten1-31* exhibited strong synthetic interactions with *fcp1-1*, a mutation in the RNA Pol II CTD-Ser2P phosphatase,

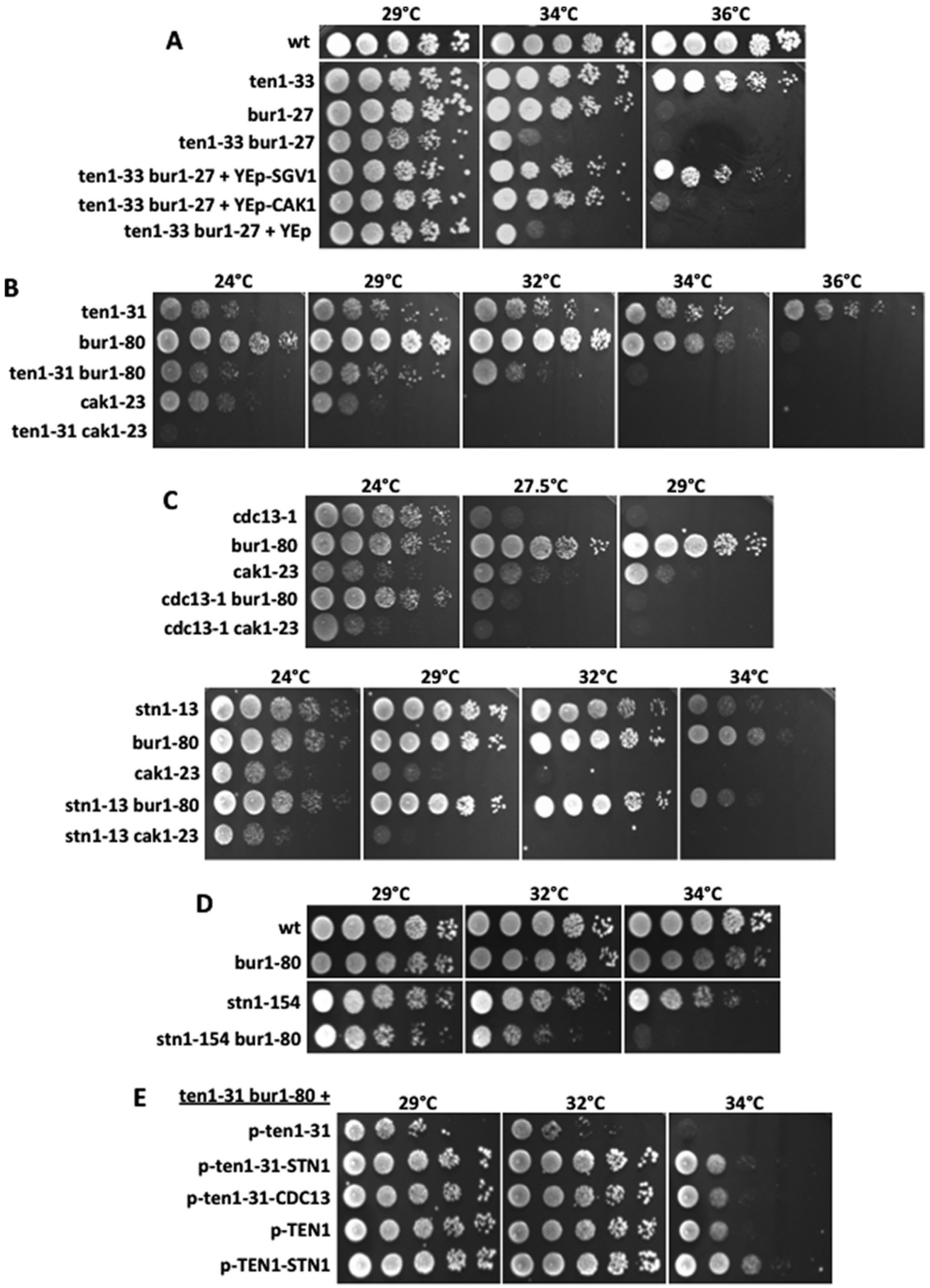

Figure 1. Genetic interactions between CST and the RNA Pol II transcriptional machinery. (**A**) The *ten1-33* mutant exhibits synthetic growth defects in combination with *bur1-27*, as seen when comparing row 2, *ten1-33*, with row 4, *ten1-33 bur1-27*. The aggravated growth defect of the *ten1-33 bur1-27* double mutant could be complemented by overexpressing either *SGV1*/*BUR1* (row 5) or *CAK1* (row 6) from a YEp24 genomic library (YEp: episomal, 2μ, plasmid); in row 7, the double mutant contains vector alone as a control. Row 3 illustrates the temperature-sensitivity defect at 36°C of *bur1-27* alone. (B–D) *BUR1*-CST and *CAK1*-CST genetic interactions. (**B**) Genetic interactions between *TEN1* and *BUR1*, as well as between *TEN1* and *CAK1*, were observed as synthetic growth defects between the temperature-sensitive corresponding mutants, *ten1-31*, *bur1-80* and *cak1-23*. Growth of the *ten1-31 bur1-80* and *ten1-31 cak1-23* double mutants was strongly impaired when compared to that of each corresponding single mutant, an effect best seen at 32 and 34°C for *ten1-31 bur1-80* and already visible at 24°C for *ten1-31 cak1-23*. (**C**) The *ten1-6*, *ten1-16*, *ten1-3* and *ten1-100* mutants also exhibited synthetic growth defects when combined with the *bur1-80* mutation, effects that were best seen at 32°C, but that somewhat differed among *ten1* mutants because of their different degrees of severity. Note that *ten1-6* and *ten1-3* are not temperature-sensitive, but yet genetically interact with *bur1-80*. (C) Absence of strong genetic interactions between *cdc13-1* and *bur1-80* or *cak1-23* (top panel)**,** as well as between *stn1-13* and and *bur1-80* or *cak1-23* (bottom panel). (**D**) The *stn1-154* mutant exhibits clear synthetic growth defects with *bur1-80*. (**E**) Synthetic growth defects of a *ten1-31 bur1-80* double mutant were rescued when either a *ten1-31-STN1* or a *ten1-31-CDC13* fusion gene was expressed from a centromeric plasmid under the control of the *TEN1* promoter (rows 1–4). Moreover, a *TEN1-STN1* fusion gene rescued *ten1-31 bur1-80* at 34°C (compare rows 1 and 5), at a higher temperature than *TEN1* alone (compare rows 4 and 5).

but not with the *rtr1*Δ or *ssu72-2* mutations, which inactivates or alters, respectively, RNA Pol II CTD-Ser5/7P phosphatases (Figure 2A and data not shown). Using classical genetic methods like those used to construct all double mutants in the present study, namely sporulation of a diploid heterozygous for both genes, we were unable to derive a *ten1-31 ctk1*Δ mutant, suggesting synthetic lethality between the two mutations. *TEN1* also genetically interacted with the elongation factors-coding *SPT4* and *SPT5* genes, as well as with *CDC73*, coding for a component of the PAF1 transcription elongation complex, and *RPB1*, coding for the largest subunit of RNA Pol II (Figure 2A). All these genetic data strongly support a role for Ten1 in RNA Pol II transcription in general, but particularly in the elongation step. Interestingly, we did not find any genetic interaction between *ten1* mutants and mutants of the THO complex, suggesting that, most probably, Ten1 is not functioning in cooperation with the THO complex to regulate transcription of non-coding telomeric DNA into TERRA (see Supplementary results and Supplementary Figure S2D and E).

To extend these genetic observations, we analysed the sensitivity of the *ten1-31* mutant to 6-azauracil (6-AU), used in the detection of transcription elongation defects (see Supplementary results and Supplementary Figure S3A). Many mutations impairing transcription elongation cause sensitivity to 6-AU, while others provide resistance to 6-AU through constitutive expression of *IMD2* (62). These particular mutations were found to cause a reduction in the RNA Pol II transcription elongation rate (50,59). We found that the *ten1-31* mutant was not sensitive to 6-AU (Supplementary Figure S3A), in agreement with the fact that *IMD2* is constitutively expressed in *ten1-31* in the absence of 6-AU and with the fact that *ten1-31* suppresses *spt4*Δ sensitivity to 6-AU (Supplementary Figure S3A). This result points again to the *ten1-31* mutation affecting transcription elongation (50,63). In addition, the *ten1-31* mutant is hypersensitive to formamide (also used to detect mRNA biogenesis defects (65), as are *cak1-23* and, to a lesser extent, *bur1-80* (Supplementary Figure S3B) (64).

It is possible that the genetic interactions between *ten1-31* and the transcription elongation mutants could be due to exacerbation of telomere defects or a combination of telomere and genome-wide defects. The data above, as well as the physical interaction between Ten1 and Spt5 (see below) indicate that this is unlikely. Moreover, although the *cdc13-1* mutant harboured more telomeric damage (under the form of abnormal levels of telomeric ssDNA) than the *ten1-31* mutant (7), it nevertheless failed to exhibit synthetic lethality with *bur1-80* (Figure 1C). Nonetheless, we analysed a few combinations of the above described mutants to see if they exhibited greater telomere structural defects than the single mutants. Specifically, we assayed for the presence of telomeric ssDNA, knowing that mutants of CST exhibit abnormal levels of telomeric ssDNA (5–7). Although the signals of telomeric ssDNA in the *ten1-31* mutant are modest compared to those in the *cdc13-1* mutant (5,7), it was nevertheless evident that the amounts of telomeric ssDNA in the *ten1-31 bur1-80* and *ten1-31 rpo21-21* double mutants and in *ten1-31* alone were quite similar, both at 24 or 32°C (Figure 2B). This strongly argues that a transcription regulatory function of CST is performed at extra-telomeric locations.

Ten1, Stn1 and Cdc13 physically and functionally interact with the Spt5 elongation factor

To examine whether Ten1 might have physical partners acting in transcription, we performed mass spectrometry analyses on a strain expressing Ten1-Myc_{13} at endogenous levels, using anti-Myc antibody. Interestingly, Spt5 was identified in three separate experiments (Supplementary Figure S4). This interaction was further corroborated by co-immunoprecipitation (co-IP) assays (Figure 3A and Supplementary Figure S5). A physical interaction between Cdc13-Myc_{13} and Spt5 was also observed, but could be detected only in one direction during co-immunoprecipitation (Figure 3A and Supplementary Figure S5), indicating that the interaction is probably rather weak. Spt5 was also identified by mass spectrometry as a potential partner of Stn1-Myc_{13} (Supplementary Figure S4). Altogether, these data allow us to conclude that Spt5 might represent a pertinent partner of the CST complex. Confirming these findings, weak genetic interactions between the temperature-sensitive *spt5-194* mutant and the temperature-sensitive *stn1-13* and *cdc13-1* mutants were observed (Figure 3B). Thus, the whole CST complex may possibly have a role in transcription elongation through interactions with Spt5.

While looking for additional clues concerning the functional interactions between Ten1 and Spt5, we observed that overexpression of *SPT5* from a 2μ plasmid rescued *ten1-31* but that, conversely, overexpression of *TEN1* (2μ plasmid) did not rescue *spt5-194* (Figure 3C). To find out whether the rescue of *ten1-31* by *SPT5* is due to a direct physical interaction between the two corresponding proteins, we again used hybrid genes, which can rescue the defect (due to a mutation) in the binding between two proteins normally physically interacting together (60,61). Interestingly, the *ten1-31-SPT5* fusion rescued *ten1-31* (Figure 3D, top panel). The rescue of *ten1-31 bur1-80* by *ten1-31-SPT5* was even more visible than that of *ten1-31* alone, due to the exacerbted temperature-sensitivity of the double mutant (Supplementary Figure S6). Very interestingly, the *ten1-31 ten1-31-SPT5* strain was no longer sensitive to formamide (Figure 3D, bottom panel). The *ten1-31-SPT4* fusion only very slightly, but reproducibly, rescued the *ten1-31* and *ten1-31 bur1-80* mutants (Supplementary Figure S6). Since Spt4 and Spt5 form a well-documented complex, this suggests that Ten1 has a privileged physical interaction with Spt5.

Table 1 summarises the genetic and physical interactions described above. Shown also in Table 1 are the interactions implicating Hmo1, Nhp6B, Pol1, Mrc1, Ctf18, Top1 and Top2, described below.

Ten1 is important to maintain proper levels of Spt5 associated to chromatin during active transcription

We performed ChIP assays in *ten1-31* and wild-type cells expressing Spt5-Flag to further investigate the interactions between CST and Spt5 (Figure 4). Spt5-Flag occupancy was significantly reduced in *ten1-31* cells compared with the wild type for all five tested genes (Figure 4A, C), while Spt5 protein levels remained unchanged (Figure 4B). It is worthy of mention that, in the *ten1-31* mutant, we clearly observed an

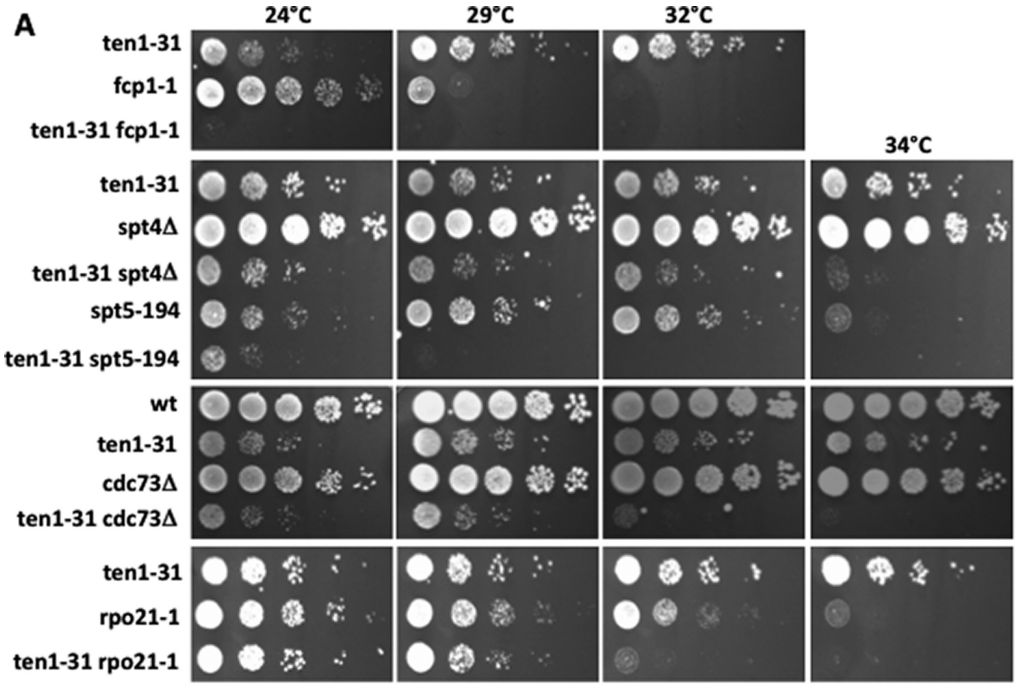

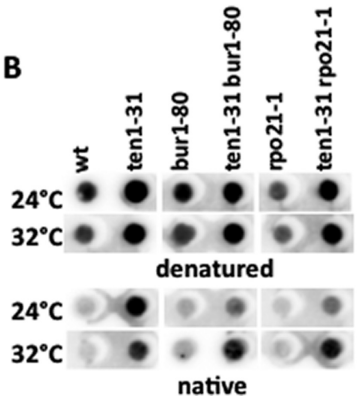

	% ssDNA at 24°C	% ssDNA at 32°C, 4 h
wt	4 ; 2	3 ; 2
ten1-31	7 ; 6	7 ; 5
bur1-80	4 ; 2	4 ; 3
ten1-31 bur1-80	6 ; 7	8 ; 6
rpo21	4 ; 3	4 ; 2
ten1-31 rpo21	6 ; 8	8 ; 5

Figure 2. Genetic and functional interactions of *ten1-31* with transcription regulators mutants. (**A**) *TEN1* geneticaly interacts with *SPT4* and *SPT5*, as well as with *FCP1*, *RPB1* and *CDC73*, as strong synthetic interactions between the corresponding mutations were observed. *ten1-31*, *spt5-194*, *fcp1-1* and *rpo21-1* (a mutation in *RPB1*) are temperature-sensitive mutations in essential genes, while *spt4*Δ and *cdc73*Δ are null mutations. (**B**) Measurements by dot blot of increased amounts of telomeric ssDNA reflecting the accumulation of telomeric DNA damage (5)**.** Left panel**:** Hybridisation of genomic DNA from the indicated mutant and wild-type (wt) strains to a TG_{1-3} ^{32}P-labelled probe under native conditions revealed the presence of abnormally high levels of telomeric ssDNA either at 24°C or 32°C, a restrictive temperature of growth for the *ten1-31*, *bur1-80* and *rpo21-1* mutations. Right panel**:** Quantification of the radioactive signals of telomeric ssDNA was performed by comparing the signal of the native dots to the corresponding signals on the denatured dots (eight times more genomic DNA was loaded on the native blots) and expressed as the percentage (% ssDNA) of signal of the denatured blot. For each temperature, numbers in the left column correspond to the signals from the blots illustrated in the left panel, while numbers in the right column represent the signals obtained in a second experiment (blots not shown). Similar results from a third experiment conducted by Southern blotting allowed us to conclude to an absence of increased telomeric ssDNA signals in the two double mutants compared with the single mutants (not shown).

increase of Spt5-Flag occupancy from the 5′-end to the 3′-end regions in the case of the extra-long *FMP27* gene, and to lesser extent in the long *YEF3* gene. This association pattern, similar to that observed for Rpb1 (see below), has been previously observed in elongation rate mutants (50,66). This also correlates with *ten1-31* cells being resistant to 6-AU treatment (Supplementary Figure S3), like some *rpb1* and transcription factors mutants in which RNA Pol II transcription elongation rate is slowed down (50,63). Our results suggest that the elongation rate might be reduced in *ten1-31* cells. Moreover, our findings are supported by the genetic interactions between *ten1* and *bur1* mutants, as Bur1 not only phosphorylates Rpb1-CTD (34), but also regulates the activity of Spt5 by phosphorylation, thus promoting transcription elongation (20).

Ten1 influences RNA Pol II occupancy during transcription

In order to further dissect the role of Ten1 in transcription, we performed chromatin immunoprecipitation (ChIP) assays to analyse RNA Pol II (Rpb1) association at several

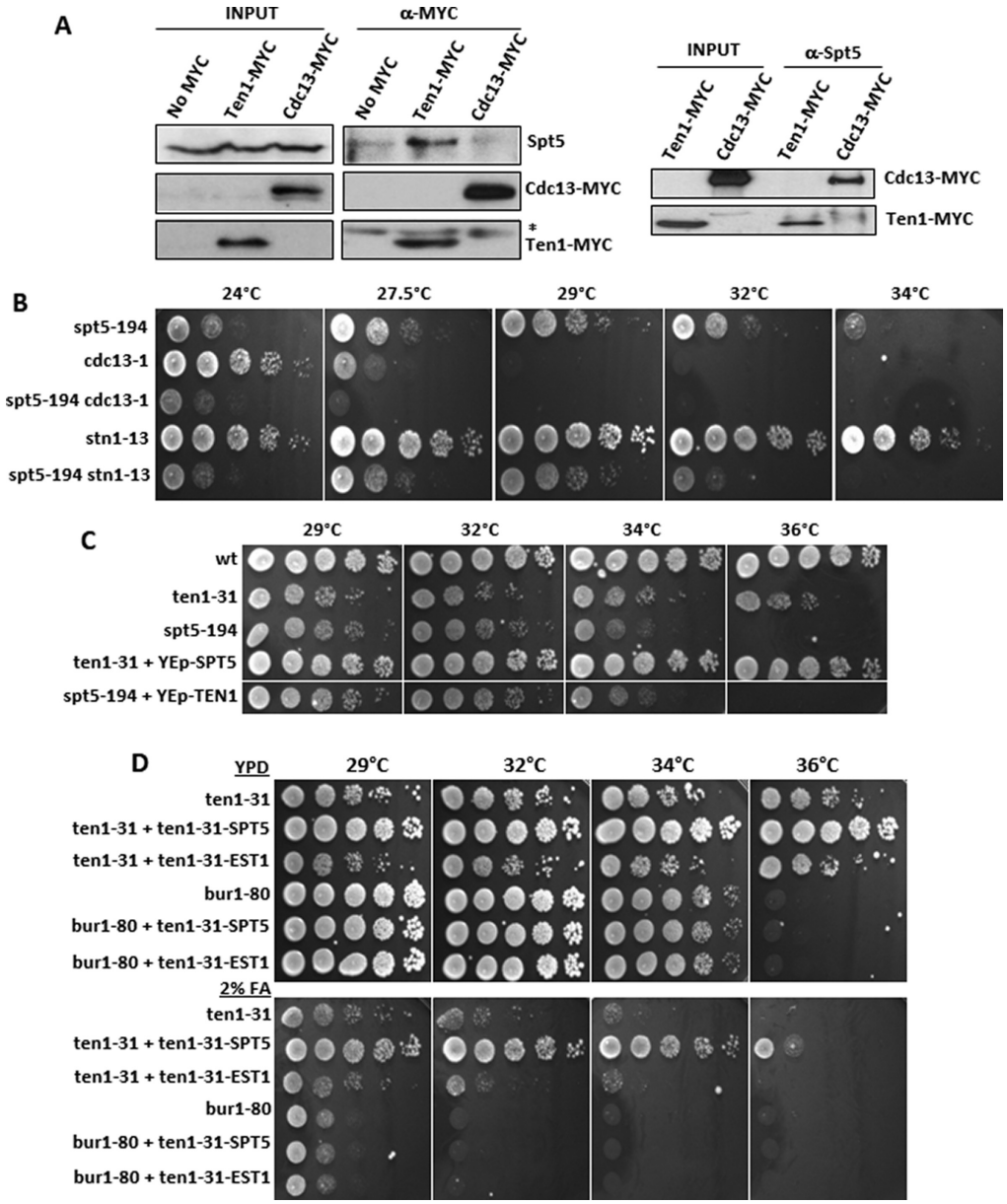

Figure 3. Ten1, but also Stn1 and Cdc13, physically and functionally interact with the Spt5 elongation factor. (**A**) Ten1-Myc$_{13}$ physically associates with Spt5 by co-IP. Cell extracts from asynchronous wild-type cells harbouring either endogenous copy of Ten1-Myc$_{13}$ or of Cdc13-Myc$_{13}$ were immunoprecipitated with either anti-Myc (left panel) or anti-Spt5 (right panel) antibody. Input and IPs were analysed by western blotting with antibodies against the indicated proteins. (* non-specific band). (**B**) Both *CDC13* and *STN1* exhibit weak genetic interactions with *SPT5*. The *spt5-194*, *stn1-13* and *cdc13-1* temperature-sensitive mutations were combined together and growth of double mutants compared with that of each single mutant at the indicated temperatures. (**C**) Overexpression of *SPT5* from a multicopy plasmid (2μ) rescues the temperature-sensitivity of *ten1-31*. (**D**) Top panel**:** A *ten1-31-SPT5* fusion rescues the *ten1-31* mutant. Bottom panel**:** The *ten1-31-SPT5* fusion rescues the sensitivity of *ten1-31* to formamide (2% FA). Hybrid genes of the indicated composition were under the control of the *TEN1* endogenous promoter in a low-copy (centromeric) plasmid. *ten1-31-EST1* provided a negative control; Est1 interacts with Cdc13 during the recruitment of telomerase to telomere ends.

regions located within three constitutively transcribed genes (*PMA1*, *YEF3* and *PGK1*) in wild-type and *ten1-31* cells at 34°C, a semi-restrictive temperature for mutant growth. We observed a significant decrease in RNA Pol II binding to all three genes tested from promoters to the 3′-end regions in *ten1-31* when compared to the wild type (Figure 5A). Similar to Rpb1, Rpb3 occupancy along the *PMA1* and *PGK1* genes was also reduced in *ten1-31* cells, as in the case of *spt5-194* cells (Supplementary Figure S7A), and this was not due to reduced levels of Rpb1 and Rpb3 proteins (Supplementary Figure S7B). A slight reduction in RNA Pol II binding was also observed in the *stn1-154* mutant at the 3′-end of the tested genes (Supplementary results and Supplementary Figure S7).

We next analysed Rpb1 distribution along the very long gene *FMP27* (8.0 Kb) whose expression was driven by the rapidly induced *GAL1* promoter, as well as along the short *GAL1* gene (1.6 kb) in the presence of galactose. In *ten1-*

Table 1. Summary of genetic and physical interactions between the CST complex and transcription or replication factors[a]

A: Data from the present study					
		Ten1	Stn1	Cdc13	Spt5
Transcription	Cak1	Synth.Gr.Def.			
	Bur1	Synth.Gr.Def.	Synth.Gr.Def.		
	Fcp1	Synth.Gr.Def.			
	Cdc73	Synth.Gr.Def.			
	Rpo21	Synth.Gr.Def.			
	Spt4	Synth.Gr.Def.			
	Spt5	Synth.Gr.Def. co-IP Fusion-Prot. Mass-Spec.	Synth.Gr.Def. Mass-Spec.	Synth.Gr.Def. co-IP	
Replication	Hmo1	Mass-Spec. co-IP	Mass-Spec.		
	Nhp6B	Mass-Spec. Mass-Spec.			
	Top1	Synth.Gr.Def.			
	Top2	Synth.Gr.Def.			
	Mrc1	Synth.Gr.Def.			
	Ctf18	Synth.Gr.Def.	Synth.Gr.Def.		
	Pol1			2-Hyb.	2-Hyb.
B: Already published relevant physical interactions[b]					
		Ten1	Stn1	Cdc13	Spt5
Replication	Pol1			2-Hyb. co-IP (73)	Mass-Spec. (22)
	Pol12		2-Hyb. (12)		
Telomere	Ten1		2-Hyb. co-IP *	2-Hyb. co-IP *	
	Stn1	2-Hyb. co-IP *		2-Hyb. co-IP *	
	Cdc13	2-Hyb. co-IP *	2-Hyb. co-IP *		

[a]Abbreviations: Synth.Gr.Def. (synthetic growth defect); co-IP. (co- immunoprecipitation); Fusion-Prot. (fusion protein); Mass-Spec. (mass spectrometry); 2-Hyb. (two-hybrid assay).
[b]Numbers report to references in the main text. * corresponds to (6,7).

31, Rpb1 occupancy at the *FMP27* gene was significantly reduced throughout the whole transcription cycle (Figure 5B). Rpb1 binding to the transcribed locus was most affected at the promoter, whereas the binding increased in *ten1-31* cells as RNA Pol II traveled through the coding region towards the 3′-end. Similar effects were observed for the *GAL1* gene (Figure 5B). These data suggest that *ten1-31* may affect not only transcription elongation, but also initiation. Altogether, our ChIP data strongly indicate that Ten1 affects RNA Pol II association to chromatin during active transcription, thus corroborating the genetic data and pointing to a role for Ten1 in transcription regulation.

A key mark of the elongation step is the phosphorylation of the Rpb1-CTD Ser2 residues. Ser2 phosphorylation starts upon promoter clearance and increases all along the transcription cycle until the polymerase reaches the termination region (27,28). Since our data suggest that Ten1 influences transcription elongation, we examined the levels of Rpb1-Ser2P associated to the chromatin during active transcription in *ten1-31* and wild-type cells. As shown in Figure 5C, Rbp1-Ser2P binding in *ten1-31* is altered when compared to wild-type cells, in accordance with an elongation defect. Whereas in the *PMA1* gene, Rpb1-Ser2P binding decreases from early elongation (5′) to termination (3′), it is increased at the 5′ region of *YEF3,* and to a lesser extent at that of *PGK1*. In these two genes, Ser2P binding is reduced in coding and 3′-end regions, similarly to our observations in the *PMA1* gene. Rpb1-Ser2P binding is also significantly reduced along the galactose inducible genes, *FMP27* and *GAL1* (Figure 5D). However, the reduction of Rpb1-Ser2P levels is not as pronounced as that of Rpb1 levels. This agrees with Ser2P levels in whole cell extracts being slightly augmented in *ten-31* cells, without changes in Rpb1 levels (Supplementary Figure S7B). Supplementary Figure S8A, B gives the ChIP Rpb1-Ser2P/Rpb1 ratios for all tested genes in *ten1-31* and the wild-type, permitting a better appreciation of the fact that Rpb1-Ser2P relative levels in *ten1-31* cells were slightly increased all over the coding region in the *FMP27* and *GAL1* genes, and clearly increased in the 5′ region of the *YEF3* and *PGK1* genes. These data indicate that changes in Ser2P profiles in *ten1-31* cells may be gene dependent. Moreover, they are consistent with the genetic interaction found between *TEN1* and *BUR1*, because the elongating kinase Bur1 specifically phosphorylates Ser2 near the promoter regions (34). They are also supported by the observation that *TEN1* genetically interacts with *FCP1*, coding for the Rpb1-Ser2P phosphatase. In summary, these RNA Pol II ChIP data support, once again, a role for Ten1 in regulating transcription elongation.

Ten1 influences RNA Pol II genome-wide distribution

In order to extend our findings and obtain a wider view of *ten1-31* transcription effects, we performed ChIP-seq experiments in which we immunoprecipitated Rpb1 or Rpb1-Ser2P in wild-type (*wt*) and *ten1-31* cells. As shown in Figure 6A, B, the Rpb1 and Ser2P association patterns (IP/INPUT ratios) with protein coding genes in both strains are similar in shape but with different binding values. This was made clearer when the *ten1-31*/wt ratios were represented (Figure 6C, D). The average Rpb1 occupancy profile in the *ten1-31* mutant shows a decreased level of binding

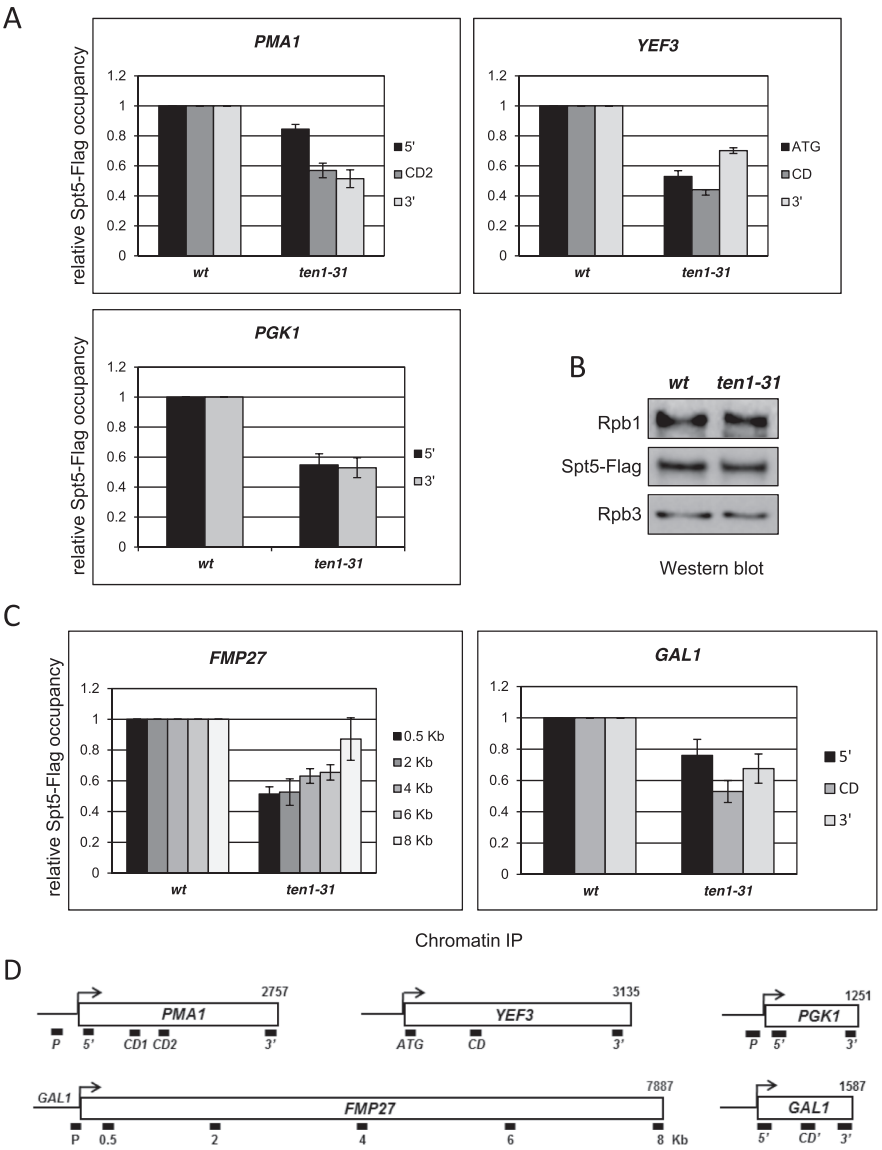

Figure 4. Ten1 is important to maintain proper levels of Spt5 associated to chromatin during active transcription. ChIP analyses were performed using *wild-type* (*wt*) and *ten1-31* strains grown at 34°C, either (**A**) in a medium containing glucose to analyse Spt5-Flag binding to the constitutively expressed genes, *PMA1*, *YEF3* and *PGK1* or (**C**) in a medium containing galactose to analyse Spt5-Flag binding to the inducible *GAL1-FMP27* and *GAL1* genes. Spt5-Flag binding was examined by qPCR and relative Spt5 binding values obtained in *ten1-31* cells are plotted relative to those in *wt* cells (set equal to 1) for each region. The data plotted here correspond to mean values from at least three independent experiments, and the error bars represent standard errors. (**B**) Spt5 total protein levels are not altered in *ten1-31* mutant cells. Levels of Spt5-Flag were analysed by western blotting using whole cell extracts from wild-type (*wt*) and *ten1-31* cells expressing Spt5-Flag. Levels of Rpb1 and Rpb3 were also tested. (**D**) Schematic representation of the analysed genes and the position of the primers used for ChIP-qPCR.

at 5′ ends, accompanied by an accumulation in the central part of the gene body together with an increased presence of Ser2P binding (Figure 6C). Figure 6D represents the ratio of Rpb1-Ser2P/Rpb1 occupancy in *ten1-31* compared to wild type. In fact, analysis of genes according to their length indicated that the defect in Ser2P phosphorylation is acquired progressively along the coding region, suggesting that Ten1 loss of function provokes an increasing defect on Rpb1-CTD phosphorylation during elongation (Supplementary Figure S9). Overall, comparison of Rpb1 binding at the *PMA1*, *YEF3* and *PGK1* genes by ChIP-seq (Supplementary Figure S11) and ChIP-qPCR (Figure 5 and Supplementary Figure S8) indicated similar types of defects. We note that the examples of single-gene ChIP-qPCR analysis given in Figure 5 and Supplementary Figure S7 did not reflect the average profile shown in the metagene analysis of Figure 6. This can be explained, however, by the fact that the metagene profile is the average of all genes, including both those which exhibited a reduction in RNA Pol II binding and those that experienced increased binding.

Having shown a general defect in Rpb1 binding all over the genome of the *ten1* mutant, we next attempted to evaluate its consequences on global gene expression through RNA-seq analysis (Supplementary Figure S12). The global

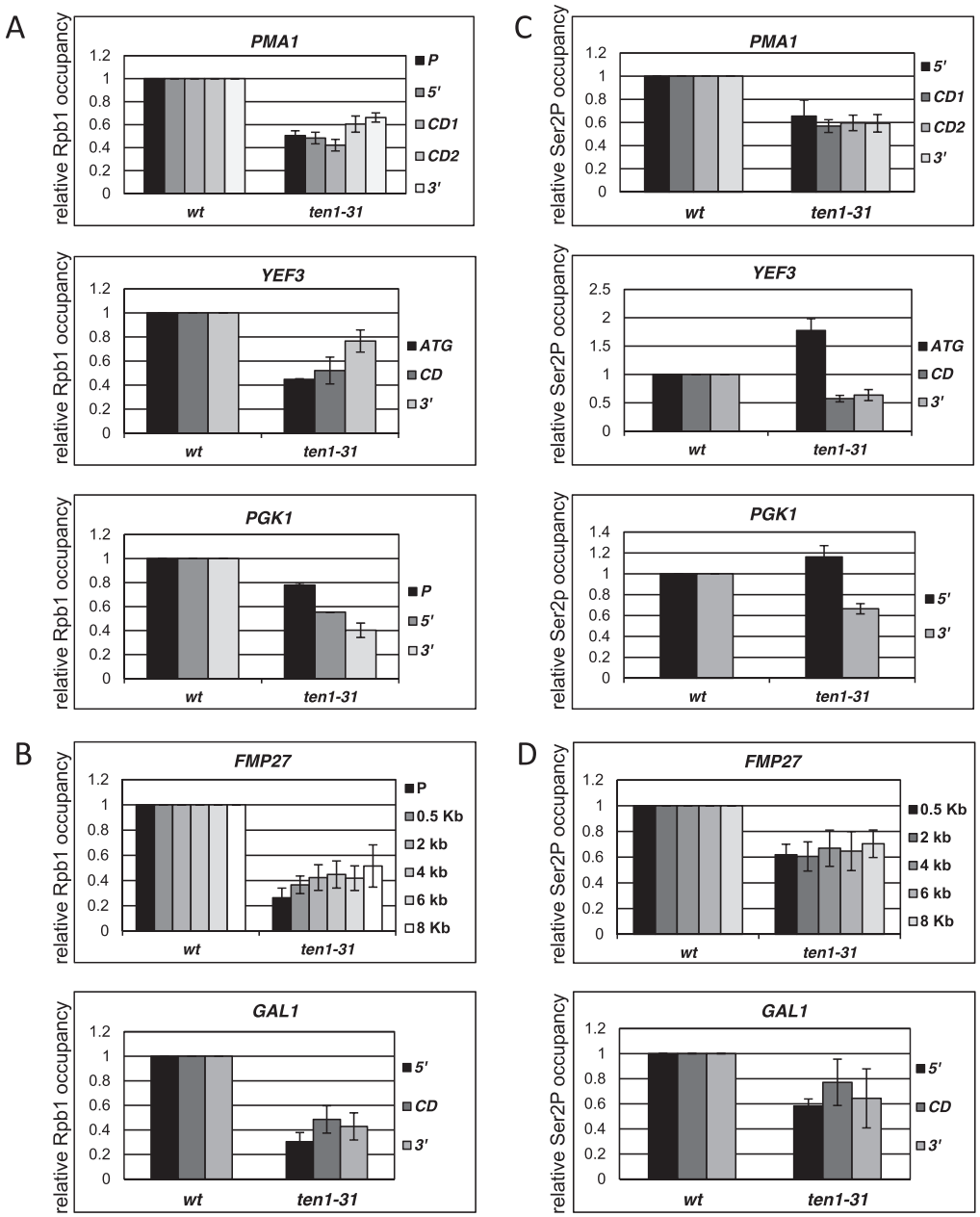

Figure 5. Ten1 influences RNA Pol II occupancy during transcription. (A, B) Rpb1 gene occupancy is reduced in *ten1-31* cells. ChIP analyses were performed in wild-type (*wt*) and *ten1-31* strains grown at 34°C, using an anti-Rpb1 antibody (8W16G). (**A**) Rpb1 occupancy at the promoter (P) or start site (ATG), coding (CD1 and CD2) and 3′-end region (3′) of three constitutively expressed genes, *PMA1*, *YEF3* and *PGK1* were examined by qPCR and quantified (see Materials and Methods). (**B**) Upper panel: Analysis of Rpb1 occupancy at the promoter (P) and all along coding region of the long gene *FMP27*, expressed under the crontrol of *GAL1* promoter. Lower panel**:** Analysis of *GAL1* gene occupancy by Rpb1 in 5′ coding and 3′-end regions. In both experiments, cells were grown in YPGal medium. (**C**) Levels of Rpb1-Ser2P are altered in *ten1-31* cells. Analysis of Rpb1-CTD Ser2P occupancy at *PMA1*, *YEF3* and *PGK1* genes by ChIP-qPCR using anti-Ser2P antibody (3E-10). (**D**) Rpb1-Ser2P occupancy at *FPM27* and *GAL1* genes. In A-D, relative Rpb1 or Rpb1-Ser2P binding values obtained in *ten1-31* cells were plotted relative to those from *wt* cells (set equal to 1) for each region. The data plotted here correspond to mean values from at least three independent experiments, and the error bars represent standard errors.

transcriptome shows a clear environmental stress response (ESR) pattern (67) with Ribosome Protein (RP) genes being down-regulated and stress-induced genes up-regulated (Figure 6G). Our transcriptomic data indicate that genes that were down-regulated (<1.5 times) in the *ten1-31* mutant exhibited less Rpb1 and Rpb1-Ser2P occupancy, as determined by ChIP-seq (Figure 6E, F), than the average genome level. In contrast, *ten1-31* up-regulated genes (>1.5 times) had more binding of Rpb1 and Rpb1-Ser2P than average. Of note, *ten1-31* S-phase regulated genes (68) were slightly below the average genome level in terms of Rpb1 and Rpb1-Ser2P occupancy.

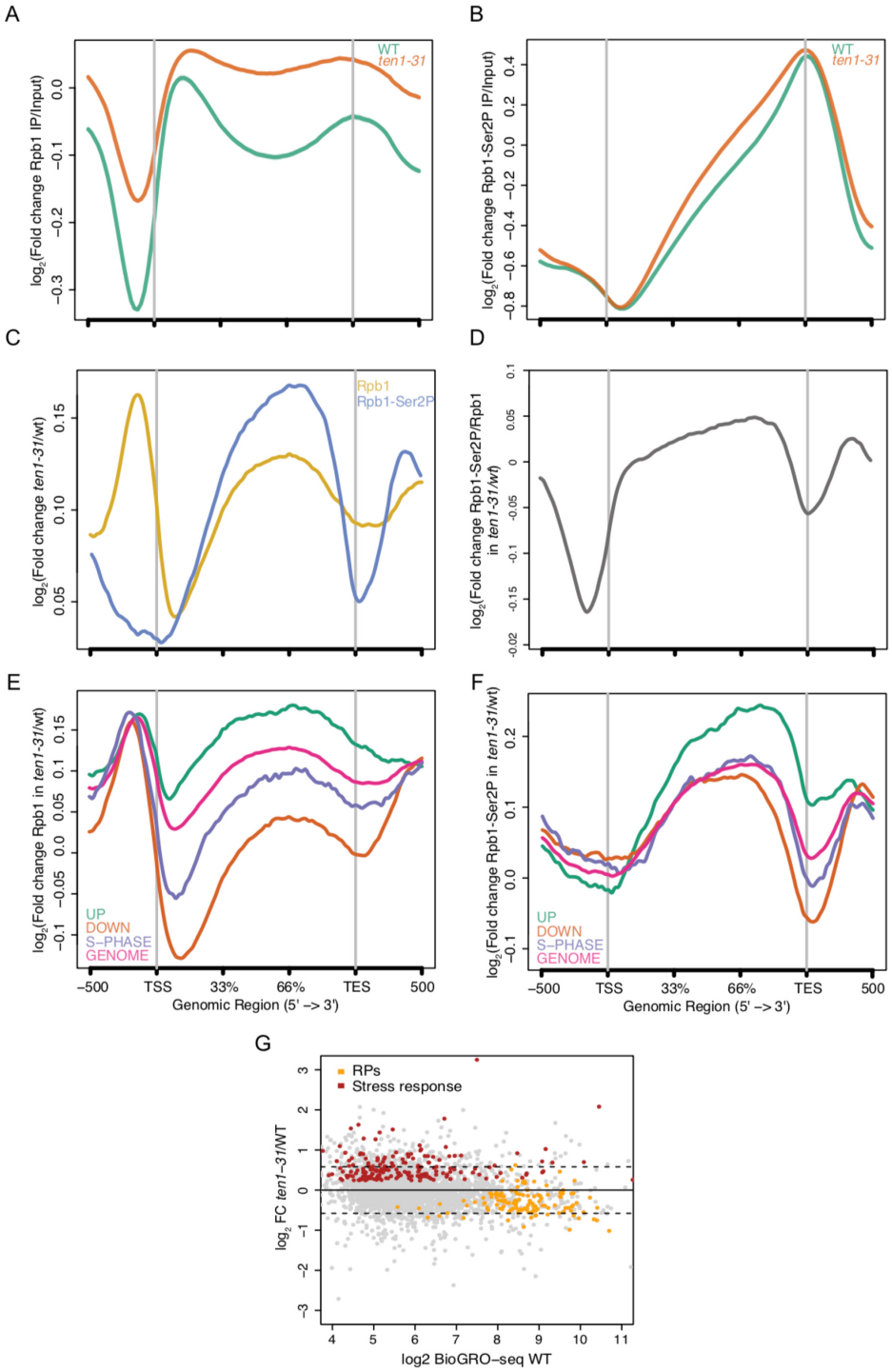

Figure 6. ChIP-seq and RNA-seq analysis of the effects of *TEN1* genetic inactivation. (**A**) Input-normalised average Rpb1 occupancy profile relative to the transcription start site (TSS) and transcription end site (TES) for all annotated protein-coding genes in the yeast genome. The green trace corresponds to the Rpb1 occupancy in the wild-type strain (*wt*), whereas the orange trace corresponds to the occupancy in the *ten1-31* mutant. The gene body regions have been scaled to an average length and depicted as percentage of the distance from the start, whereas the upstream and downstream flanking regions represent real genomic distances from the TSS and the TES. Normalised occupancy is represented as the $\log_2$ Fold Change of Rpb1 IP divided by its corresponding Input. (**B**) Same as in (A) for the Rpb1-Ser2P IP/Input. (**C**) Average binding profiles for both Rpb1-IP/Input and Rpb1-Ser2P-IP/Input, as indicated, in *ten1-31* (values normalised to the *wt*). (**D**) Ratio of Rpb1-Ser2P/Rpb1 average occupancies in *ten1-31*/*wt*. (**E**) Same as in (C) for different gene subgroups compared to the average of the genome. 'Down' are the down-regulated genes found in the differential expression analysis of the transcriptome *ten1-31*/*wt* (n = 982). 'Up' are the up-regulated genes ($n = 980$). 'S phase' are differentially expressed genes which have a peak of expression in S phase ($n = 282$). (**F**) Same as in (E) for the Rpb1-Ser2P. (**G**) MA plot showing the results of the DESeq2 differential expression analysis of the *ten1-31* mutant/wt relative to the mean transcription rate level of each gene in both conditions. BioGROseq data from wild type (WT) cells were used as a measure of nascent transcription rate (Jordán-Pla *et al.*, unpublished). Horizontal dashed lines indicate the differential expression cut-off chosen to call genes as up- or down-regulated in our analysis.

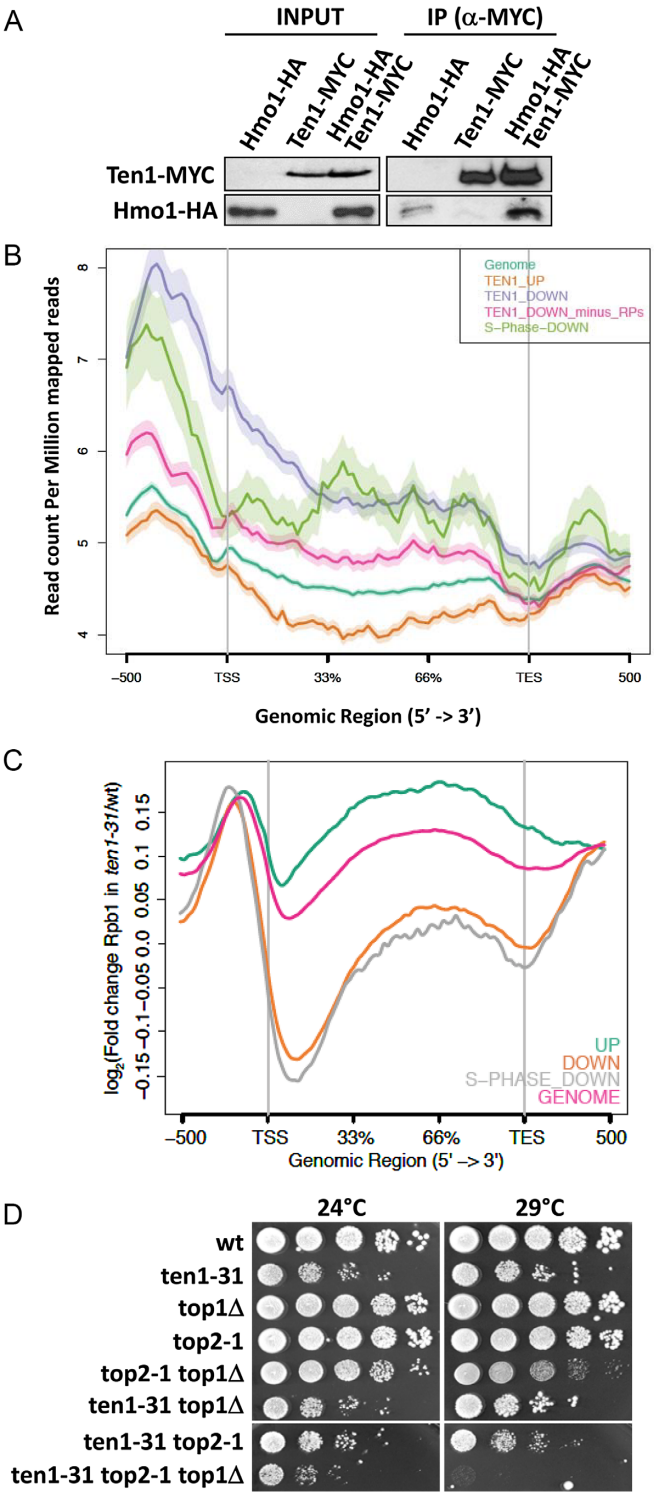

Figure 7. Hmo1 interacts with Ten1 and binds to promoters and gene bodies of genes silenced upon *TEN1* genetic inactivation. (**A**) Ten1-Myc$_{13}$ associates with Hmo1-HA$_2$ as determined by co-IP. The assay was performed on whole cell extracts from Hmo1-HA$_2$, Ten1-Myc$_{13}$, and Hmo1-HA$_2$ Ten1-Myc$_{13}$ cells using an anti-Myc antibody. Inputs and IPs were analysed by western blotting with antibodies directed against the indicated proteins. (**B**) ChIP-exo Hmo1 occupancy profile relative to the TSS and TES sites for different subsets of genes compared to the average of the genome. 'TEN1_DOWN' represents the down-regulated genes found in the differential expression analysis of the transcriptome *ten1-31*/wt (n = 982). 'TEN1_DOWN_minus_RPs' represents the *ten1-31* down-regulated genes after removing ribosomal protein genes ($n = 899$). 'TEN1_UP' represents the genes up-regulated in *ten1-31* ($n = 980$). 'S-Phase-DOWN' represents the genes that have a peak of expression in the S phase and are down-regulated in *ten1-31* ($n = 154$). Standard deviations are represented as translucent areas around the solid traces. (**C**) RNA Pol II occupancy (Rpb1 ChIP-seq) profiles relative to the TSS and TES sites for different subsets of genes compared to the average of the genome. In this figure, the 'UP' and 'DOWN' traces represent the genes that were found to be up-regulated and down-regulated, respectively, in the differential expression analysis of the transcriptome *ten1-31*/wt ($n = 980$ and $n = 982$, respectively), compared with the expression of the whole genome (6600 genes, 'GENOME'). 'S-PHASE_DOWN' represents RNA Pol II occupancy of the 154 genes with a peak expression in S phase that were found to be down-regulated in *ten1-31*. Note that all traces represent levels of occupancy in the *ten1-31* mutant compared with the wild-type (*wt*) after each has been normalised to input. (**D**) *TOP1* and *TOP2* genetically interact with *TEN1*, but only when both *TOP1* and *TOP2* have been mutated. The *top1*Δ and temperature-sensitive *top2-1* mutants were used. Growth of the *ten1-31 top2-1 top1*Δ triple mutant was clearly impaired when compared to that of each corresponding single or double mutants.

A subset of S-phase expressed genes are regulated by Ten1 in concert with Hmo1

Besides Spt5, our mass spectrometry experiments identified two proteins that were isolated four times: in all three different experiments using Ten1-Myc$_{13}$ as the bait and in one experiment using Stn1-Myc$_{13}$ as the bait. These proteins are Hmo1 and Nhp6B (Supplementary Figure S4), both previously implicated in transcription regulation (69,70). The interaction between Ten1-Myc$_{13}$ and Hmo1-HA$_2$ was confirmed by co-IP (Figure 7A). Since, as mentioned above for *ctk1*Δ, numerous attempts to derive a *ten1-31 hmo1*Δ double mutant failed, it is possible that the functional interactions between Ten1 and Hmo1 are so strong that loss of function of both cannot be tolerated by the cell.

This raises the question of whether the pattern of Hmo1 binding genome-wide is altered in *ten1-31* cells. According to ChIP-exo data, Hmo1 tends to accumulate at promoter regions of target genes (55). In addition, Hmo1 was found to be preferentially recruited at Top2-bound regions of S phase-arrested cells, principally, but not exclusively, at gene promoters. Hmo1 and Top2 were proposed to prevent damage at sites of S phase transcription upon collision with an incoming replication fork (37). Re-examination of Hmo1 ChIP-exo data from Reja *et al.* (55) revealed that *ten1-31* down-regulated S phase genes bind Hmo1 at a higher level than the average of the genome (Figure 7B). Moreover, the whole set of *ten1-31* down-regulated genes exhibited even higher Hmo1 binding, while up-regulated genes were on average less bound by Hmo1 than at genome-wide level (Figure 7B). Even after subtraction of RP genes from the list of *ten1-31* down-regulated genes (because RP genes have a very high level of Hmo1 occupancy (55), we could still observe that all *ten1-31* down-regulated genes bound Hmo1 to a higher extent than genome average (Figure 7B).

Interestingly, among the 877 genes (out of a total of 6600) that have a peak of high expression in S phase (68), there was a statistically significant overlapping (P-value 9×10^{-4}) with the 1962 genes differentially expressed in the *ten1-31* mutant. Starting with the total number of S phase genes differentially expressed in *ten1-31* (282 out of a total of 877),

we calculated the overlap between the genes up-regulated in *ten1-31* and those that are expressed in S phase. This overlap (128 genes) was found to be non-significant (*P*-value < 0.434). However, when this was done for the *ten1-31* down-regulated genes *versus* those expressed in S phase we did observed a significant overlap (154 genes; *P*-value < 0.01).

Interestingly, after comparing our genome-wide analyses by ChIP-seq and RNA-seq, we found, as illustrated in Figure 7C, that *ten1-31* down-regulated S phase genes were even more depleted of RNA Pol II (Rpb1 occupancy) than the average of all *ten1-31* down-regulated genes. Therefore, we conclude that the group of *ten1-31* differentially-expressed genes (that preferentially bind Hmo1 at their promoters) exhibits a deficit in RNA Pol II occupancy.

Previous work has uncovered functional interactions between Hmo1 and both Top1 and Top2 at gene promoters of S-phase arrested yeast cells (37). Interestingly, the *ten1-31 hmo1*Δ double mutant was inviable and the *ten1-31* mutant exhibited synthetic interactions with the *top1*Δ *top2-1* double mutant (Figure 7D).

MRC1 and *CTF18*, coding for DNA replication damage sensing proteins, genetically interact with *TEN1* and *STN1*

Based on these findings (summarised in Supplementary Figure S13A and Table 1), we wondered whether there might be a specific context where CST might bind and affect RNA Pol II. Human STN1 and CTC1 were first isolated in biochemical experiments as alpha accessory factors, AAF-44 and AAF-132, respectively, of the DNA polymerase α complex (71,72). Although it has been known for some time that Cdc13 physically interacts with Pol1, the largest subunit of the DNA Pol α complex (73), and Stn1 with Pol12, a subunit of DNA Pol α (12), it is not known where exactly these interactions take place (at the telomeres or at the replication forks or both?). We speculated that CST is normally present at the replication fork and that potential collisions between the moving fork and an incoming transcription unit might activate DNA replication checkpoint proteins. Ctf18 and Mrc1 are, together with Mec1 and Rad53, the most important actors in maintaining replication fork integrity upon DNA replication stress (74). If CST responds to such a stress to affect transcription accordingly, then mutations in CST might be synthetically lethal with mutations in *MRC1* or *CTF18*. Indeed, strong genetic interactions between *CTF18* and *TEN1*, *CTF18* and *STN1*, as well as between *MRC1* and *TEN1*, were observed (Figure 8A). These results suggest that CST functions in transcription regulation might take place at the replication fork. In support for the assumption that transcription units might be regulated at the replication forks, at least under particular circumstances, we could detect physical interactions between Pol1 and Spt5 by two-hybrid (Figure 8B).

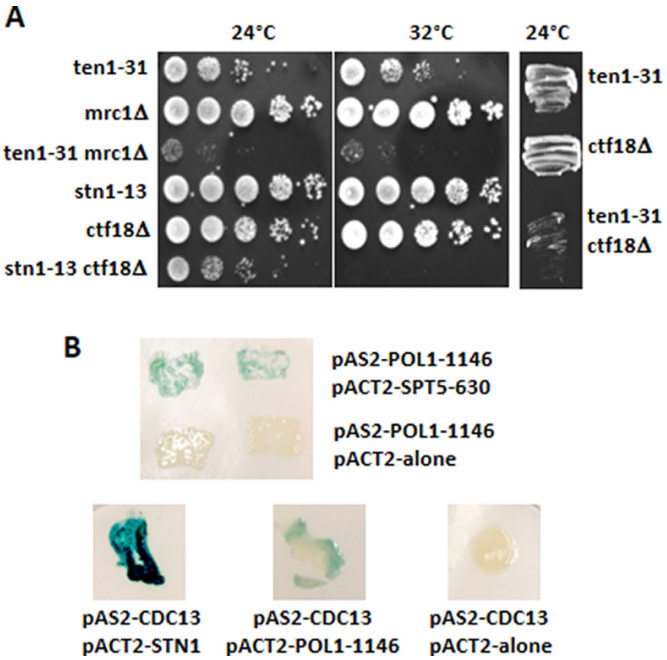

Figure 8. Genetic and physical connection of CST to DNA replication. (**A**) *ten1* and *stn1* mutants are sensitive to DNA replication stress. Genetic interactions between mutations in CST components, *ten1-31* and *stn1-13*, and null mutations in the DNA replication stress checkpoint genes *MRC1* and *CTF18*. (**B**) Two-hybrid interactions between Pol1 and Spt5, as well as between Cdc13 and Stn1 or Pol1. In top panel, Y190 strains simultaneously expressing pAS2-POL1-first 1146 nt and pACT2-SPT5-first 630 nt (top row) or pACT2 alone (botton row) were positive for β-galactosidase activity in the X-gal assay, as were cells coexpressing pAS2-CDC13 and pACT2-STN1 or pACT2-POL1–1146, unlike those expressing pACT2 alone, used here as negative control (bottom panel). Patches of cells replica-plated on nitrocellulose membrane were incubated for 2 h at 30°C and then photographed.

DISCUSSION

Ten1 has a function in transcription elongation in association with Stn1 and Cdc13

Several sets of data demonstrate that Ten1 functions in regulating RNA Pol II transcription in association with Stn1 and Cdc13, the three proteins forming the essential *S. cerevisiae* telomeric CST complex. First, Ten1 influences association of Spt5, a major, highly conserved player in transcription elongation, with actively transcribed chromatin, as well as RNA Pol II distribution during the whole transcription cycle. We also show that Cdc13 and Stn1 physically associate with Spt5 and genetically interact with it. Second, Rpb1 and Rpb1-Ser2P levels, which are crucial to correctly maintain transcription elongation, are also altered in the *ten1* mutant. Consistent with this, *ten1-31* genetically interacts with the CTD-Ser2P phosphatase, Fcp1, and the CTD-Ser2P kinase, Bur1, as well as with the Spt4/5 and Cdc73 elongation factors. Concordantly, *ten1-31* displayed 6-AU resistance, a feature common to mutations causing a decrease in elongation rate (50,63,75). Third, our experiments with the *ten1-31-STN1* and *ten1-31-CDC13* hybrid genes suggest that all three components are acting together to regulate transcription. Actually, the *stn1-154* mutant exhibited genetic interactions with *bur1-80* and conferred mild defects in the association of RNA Pol II with the 3′-end region of long genes. Finally, the CST complex seems to specifically participate in RNA Pol II transcription, as we have not observed that the *ten1-31* mutation affects at least RNA Pol I association to the rDNA genes (Supplementary Figure S14).

One could argue that the role of Ten1 in transcription proposed here might just be indirect and/or non-specific. It might potentially result from the lethal combination of a stress response triggered when Ten1 is defective and the transcriptional stress provoked by inactivation of Bur1 or other RNA Pol II-associated function. However, this is highly improbable for several reasons. First, the *cdc13-1* mutant displayed no genetic interaction with *bur1-80*; yet this mutant has the most severe telomeric phenotype among all *cdc13*, *stn1* and *ten1* mutants described to date (5,7). Therefore, the strong genetic interaction observed between *ten1-31* and *bur1-80* can only be due to Ten1 having a more important role in transcription regulation than Stn1 and Cdc13. Second, *ten1* mutants with telomeric phenotype but a much less severe morphological phenotype than *ten1-31*, such as *ten1-3*, *ten1-6* or *ten1-100* (7), nevertheless exhibited synthetic growth defects in combination with *bur1-80*. This strongly points out to the existence of specific genetic interactions between *ten1* and transcription mutants and eliminates the possibility of non-specific effects due to general loss of fitness. Third, the existence of physical interactions between Spt5 or Hmo1 and Ten1 or Stn1, which like several other telomeric proteins are proteins with extremely low intracellular amounts (https://www.yeastgenome.org/locus/S000002489/protein), is incompatible with the hypothesis of non-specific genetic interactions between the corresponding mutants. This view is supported by the observation that the Ten1-31-Spt5 fusion rescued *ten1-31*. Fourth, our experiments with hybrid genes reveal a unique relationship between telomeric and transcription pathways, namely the rescue of the loss of function of the *BUR1* kinase by slight overexpression of a *TEN1-STN1* fusion. Again, this cannot be explained by the existence of non-specific effects between two unrelated pathways.

This more important role of Ten1 in transcription regulation, compared with those of Stn1 and Cdc13, was confirmed by the finding that the physical interaction between Cdc13-Myc and Spt5 was even weaker than that between Ten1-Myc and Spt5. The actual participation of Cdc13 and Stn1 in the regulation of transcription, suggested by physical association of Cdc13 and Spt5, as well as by that between Stn1 and Spt5 (and Hmo1) detected by mass spectrometry, was confirmed by the experiments using the *ten1-31-STN1* and *ten1-31-CDC13* hybrid genes. These experiments suggest that a fully assembled CST complex is needed for optimal transcription regulation under certain circumstances, but that the interface between Ten1 and the transcriptional machinery prevails. Cdc13 and Stn1 might on the other hand control other essential key steps, potentially upstream, for instance to relay damage or defects that will necessitate the intervention of CST in the control of transcription regulation. A possible scenario for such events is proposed below.

Does CST have a potential role in stimulating the transcription machinery upon collision with a replication fork?

Our working model starts with the likely possibility that CST action on transcription may be initiated at the progressing replication fork (Supplementary Figure S13B). We speculate that, upon torsional stress provoked by the imminent arrival of a moving transcription unit in front of the progressing replication fork, the checkpoint sensors Ctf18 and Mrc1 (and also Mec1 and Rad53, the effectors of both sensors) arrest the progression of the replication fork (among other events). A transient dissociation between Cdc13 and Pol1 and/or Stn1 and Pol12, both components of the DNA Pol α complex then allows CST to move towards the colliding transcription unit and establish contacts with Hmo1 (Supplementary Figure S13B). Supporting this hypothesis, we have found physical interactions between Pol1 and Spt5 by two-hybrid, confirming a similar interaction detected by mass spectrometry (22).

Recent findings have established that in S-phase arrested cells, Hmo1 was preferentially recruited at Top2-bound regions, principally at gene promoters. This led to the proposal that Top2 (and also Top1) and Hmo1 might solve difficult topological contexts in S phase when transcription has to face incoming replication forks (37). Top1, Top2 and Hmo1 (37), together with Sen1 (76), appear to be sufficient to manage head-on collisions between the transcription and replication machineries. We propose, based on our finding that Hmo1 occupancy is higher than average at *ten1-31* down-regulated genes, that the CST complex might play an important role in stimulating the RNA Pol II machinery, principally through physical interactions with Spt5, after it has collided with the replication fork or, at least, in synchronizing both machineries (Supplementary Figure S13B). Interestingly, our data suggest the existence of functional interactions between Ten1 and the three proteins implicated in managing transcription/replication collisions, Hmo1, Top1 and Top2 (37). In fact, if Ten1 role is to limit the fatal consequences of collisions between the RNA and DNA polymerases, then one should expect that the effects of its inactivation on gene expression would be most apparent when DNA replication is taking place. Our data indicate that this might be the case, as genes down-regulated in the *ten1-31* mutant were highly enriched in S phase-transcribed genes.

Budding yeast CST might also stimulate DNA Pol α activity after the collision, as proposed for mammalian CST in face of a DNA replication stress (14,15). In our model, yeast CST travels with the replication forks and arrives at the extremities of the telomeres at the right time, during late S phase, to occupy the elongating single-stranded G-overhang (77). This way, CST having accomplished its functions of transcriptional regulation during S phase executes its telomeric functions immediately after (Supplementary Figure S13B).

The situation with Ten1 described here bears striking resemblances with that concerning Hog1. Upon osmostress, the Hog1 MAP kinase interacts with components of the RNA Pol II transcription elongation complex (such as Spt4, Paf1, Dst1 and Thp1) to recruit the RSC chromatin remodeler complex to stress-responsive genes (78,79). Bearing similarities with this situation, Ten1 is functionally linked to Spt5 and genetically linked to Cdc73, a subunit of the PAF1 complex (20). Therefore, the Spt4/5 and PAF1 complexes might represent a privileged location within the RNA Pol II transcription machinery to regulate transcription upon either external stress or stress provoked by fork progression.

Other telomeric proteins are also known to play a role in transcription. For instance, in mouse embryonic cells and

human cancer cells, RAP1 and TRF2 endorse extratelomeric functions and are true regulators of transcription (80–82). *S. cerevisiae* Rap1, another telomeric protein, is also a true transcription factor as it modulates expression of many genes, including ribosomal protein genes, MATα genes, several glycolytic enzyme genes (83), as well as genes that adapt chromatin changes in response to telomeric senescence (84).

Intriguingly, several *S. cerevisiae* mutants of factors involved in RNA Pol II transcript biogenesis have been found to exhibit altered telomere length (85). It has been argued that, since telomerase and most of its regulators are present in the cell at extremely low amounts, even slight changes in transcription regulators might significantly affect telomere length (85). Alternatively, these transcription mutants might necessitate increased levels of CST proteins to manage head-on collisions, resulting in a deficit of telomeric CST affecting telomere length.

In summary, the present data uncover a completely novel facet of the telomeric Cdc13–Stn1–Ten1 complex in the regulation of transcription, serving to optimize the functioning of the RNA Pol II machinery upon head-on collision with a replication fork following signaling by Hmo1. Noticeably, in our model, CST might also be in charge of coordinating the completion of S phase with the onset of telomere replication by telomerase/Pol α. Therefore, the CST complex now appears as a versatile machine with several distinct functions that take advantage of the properties of each of its three components at different times of the cell cycle and are based on several different protein-protein interactions, principally with Pol1, Pol12, Est1 and, as shown here, Spt5, as well as on the ssDNA-binding properties of Cdc13 and Stn1. Additionally, a well established role of Spt5 is to release paused or arrested RNA Pol II and promote transcription elongation in higher eucaryotes (17). Therefore, based on our data, it is possible that Spt5 might also be acting to promote the release of paused or arrested RNA Pol II from sites where the transcription and replication machineries are prone to collide. The present finding of the existence of extra-telomeric functions for Ten1 in the regulation of RNA polymerase II in cooperation with Stn1 and Cdc13 has profound repercussions on future studies both on telomeric and transcription pathways.

DATA AVAILABILITY

Raw and processed genomic data are available at GEO under the accession number GSE120296.

SUPPLEMENTARY DATA

Supplementary Data are available at NAR Online.

ACKNOWLEDGEMENTS

We are grateful to Alberto Paradela and Adán Alpízar Morúa from the Proteomic Department at the CNB, CSIC Madrid, Spain, for help with the mass spectrometry experiments. We thank people at the Genomic Facility at the CRG in Barcelona. We also thank David Lydall, Craig Peterson, Rolf Sternglanz and Steve Elledge for the gift of strains. We also thank Charles White and Maria Gallego for helpful discussion and critical reading of the manuscript.

Authors contributions: N.G., O.C. and M.C. conceived and designed the experiments. N.G., N.G.P., E.M., O.C. and M.C. performed the experiments. A.J. and J.E.P.O. analyzed RNA-seq and ChIP-seq data. N.G., O.C. and M.C. analysed the data. N.G., O.C. and M.C. wrote the manuscript. All authors revised and approved the manuscript.

FUNDING

From the 'Fondation de France' and 'Ligue Grand-Ouest contre le Cancer' (to M.C.); Consejo Superior de Investigaciones Cientificas [i-LINK1213 to O.C. and M.C.]; Spanish Ministry of Economy and Competitiveness (MINECO) [BFU2017-84694-P to O.C., BFU2016-77728-C3-3-P to J.E.P-O.]; Generalitat Valenciana [PROMETEOII 2015/006 to to J.E.P-O.]; Spanish Excellence Network *mRNA life* [BFU2015-71978-REDT]; Program 'Escalera de Excelencia' from *Junta de Castilla y León* [CLU-2017-03], cofunded by the P.O. FEDER from *Castilla y León 14-20*. Funding for open access charge: LIGUE contre le Cancer, and MINECO (BFU2017-84694-P).
Conflict of interest statement. None declared.

REFERENCES

1. de Lange,T. (2009) How telomeres solve the end-protection problem. *Science*, **326**, 948–952.
2. Palm,W. and de Lange,T. (2008) How shelterin protects mammalian telomeres. *Annu. Rev. Genet.*, **42**, 301–334.
3. Martinez,P. and Blasco,M.A. (2011) Telomeric and extra-telomeric roles for telomerase and the telomere-binding proteins. *Nat. Rev. Cancer*, **11**, 161–176.
4. Miyoshi,T., Kanoh,J., Saito,M. and Ishikawa,F. (2008) Fission yeast Pot1-Tpp1 protects telomeres and regulates telomere length. *Science*, **320**, 1341–1344.
5. Garvik,B., Carson,M. and Hartwell,L. (1995) Single-stranded DNA arising at telomeres in *cdc13* mutants may constitute a specific signal for the *RAD9* checkpoint. *Mol. Cell Biol.*, **15**, 6128–6138.
6. Grandin,N., Reed,S.I. and Charbonneau,M. (1997) Stn1, a new *Saccharomyces cerevisiae* protein, is implicated in telomere size regulation in association with Cdc13. *Genes Dev.*, **11**, 512–527.
7. Grandin,N., Damon,C. and Charbonneau,M. (2001) Ten1 functions in telomere end protection and length regulation in association with Stn1 and Cdc13. *EMBO J.*, **20**, 1173–1183.
8. Martin,V., Du,L.L., Rozenzhak,S. and Russell,P. (2007) Protection of telomeres by a conserved Stn1-Ten1 complex. *Proc. Natl. Acad. Sci. U.S.A.*, **104**, 14038–14043.
9. Miyake,Y., Nakamura,M., Nabetani,A., Shimamura,S., Tamura,M., Yonehara,S., Saito,M. and Ishikawa,F. (2009) RPA-like mammalian Ctc1-Stn1-Ten1 complex binds to single-stranded DNA and protects telomeres independently of the Pot1 pathway. *Mol. Cell*, **36**, 193–206.
10. Surovtseva,Y.V., Churikov,D., Boltz,K.A., Song,X., Lamb,J.C., Warrington,R., Leehy,K., Heacock,M., Price,C.M. and Shippen,D.E. (2009) Conserved telomere maintenance component 1 interacts with STN1 and maintains chromosome ends in higher eukaryotes. *Mol. Cell*, **36**, 207–218.
11. Mirman,Z., Lottersberger,F., Takai,H., Kibe,T., Gong,Y., Takai,K., Bianchi,A., Zimmermann,M., Durocher,D. and de Lange,T. (2018) 53BP1-RIF1-shieldin counteracts DSB resection through CST- and Polα-dependent fill-in. *Nature*, **560**, 112–116.
12. Grossi,S., Puglisi,A., Dmitriev,P.V., Lopes,M. and Shore,D. (2004) Pol12, the B subunit of DNA polymerase alpha, functions in both telomere capping and length regulation. *Genes Dev.*, **18**, 992–1006.
13. Lue,N.F., Chan,J., Wright,W.E. and Hurwitz,J. (2014) The CDC13-STN1-TEN1 complex stimulates Pol α activity by promoting RNA priming and primase-to-polymerase switch. *Nat. Commun.*, **5**, 5762.
14. Stewart,J.A., Wang,F., Chaiken,M.F., Kasbek,C., Chastain,P.D. 2, Wright,W.E. and Price,C.M. (2012) Human CST promotes telomere

duplex replication and general replication restart after fork stalling. *EMBO J.*, **31**, 3537–3549.
15. Kasbek,C., Wang,F. and Price,C.M. (2013) Human TEN1 maintains telomere integrity and functions in genome-wide replication restart. *J. Biol. Chem.*, **288**, 30139–30150.
16. Pelechano,V., Jimeno-González,S., Rodríguez-Gil,A., García-Martínez,J., Pérez-Ortín,J.E. and Chávez,S. (2009) Regulon-specific control of transcription elongation across the yeast genome. *PLoS. Genet.*, **5**, e1000614.
17. Hartzog,G.A. and Fu,J. (2013) The Spt4–Spt5 complex: A multi-faceted regulator of transcription elongation. *Biochim. BiophysI. Acta*, **1829**, 105–115.
18. Mayer,A., Lidschreiber,M., Siebert,K., Leike,J., Soding,P. and Cramer,P. (2010) Uniform transitions of the general RNA polymerase II transcription complex. *Nat. Struct. Mol. Biol.*, **17**, 1272–1278.
19. Tardiff,D.F., Abruzzi,K.C. and Rosbash,M. (2007) Protein characterization of *Saccharomyces cerevisiae* RNA polymerase II after in vivo cross-linking. *Proc. Natl. Acad. Sci. U.S.A.*, **104**, 19948–19953.
20. Liu,Y., Warfield,L., Zhang,C., Luo,J., Allen,J., Lang,W.H., Ranish,J., Shokat,K.M. and Hahn,S. (2009) Phosphorylation of the transcription elongation factor Spt5 by yeast Bur1 kinase stimulates recruitment of the PAF complex. *Mol. Cell Biol.*, **29**, 4852–4863.
21. Zhou,K., Kuo,W.H., Fillingham,J. and Greenblatt,J.F. (2009) Control of transcriptional elongation and cotranscriptional histone modification by the yeast BUR kinase substrate Spt5. *Proc. Natl. Acad. Sci. U.S.A.*, **106**, 6956–6961.
22. Lindstrom,D.L., Squazzo,S.L., Muster,N., Burckin,T.A., Wachter,K.C., Emigh,C.A., McCleery,J.A., Yates,J.R. 3 and Hartzog,G.A. (2003) Dual roles for Spt5 in pre-mRNA processing and transcription elongation revealed by identification of Spt5-associated proteins. *Mol. Cell Biol.*, **23**, 1368–1378.
23. Eick,D. and Geyer,M. (2013) The RNA polymerase II carboxy-terminal domain (CTD) code. *Chem. Rev.*, **113**, 8456–8490.
24. Heidemann,M., Hintermair,C., Voß,K. and Eick,D. (2013) Dynamic phosphorylation patterns of RNA polymerase II CTD during transcription. *Biochim. Biophys. Acta*, **1829**, 55–62.
25. Suh,H., Ficarro,S.B., Kang,U.B., Chun,Y., Marto,J.A. and Buratowski,S. (2016) Direct analysis of phosphoryation sites on the Rpb1 C-terminal domain of RNA polymerase II. *Mol. Cell*, **61**, 297–304.
26. Schüller,R., Forné,I., Straub,T., Schreieck,A., Texier,Y., Shah,N., Decker,T.M., Cramer,P., Imhof,A. and Eick,D. (2016) Heptad-specific phosphorylation of RNA polymerase II CTD. *Mol. Cell*, **61**, 305–314.
27. Buratowski,S. (2003) The CTD code. *Nat. Struct. Biol.*, **10**, 679–680.
28. Buratowski,S. (2009) Progression through the RNA polymerase II CTD cycle. *Mol. Cell*, **36**, 541–546.
29. Hsin,J.P. and Manley,J.L. (2012) The RNA polymerase II CTD coordinates transcription and RNA processing. *Genes Dev.*, **26**, 2119–2137.
30. Meinhart,A., Kamenski,T., Hoeppner,S., Baumli,S. and Cramer,P. (2005) A structural perspective of CTD function. *Genes Dev.*, **19**, 1401–1415.
31. Phatnani,H.P. and Greenleaf,A.L. (2006) Phosphorylation and functions of the RNA polymerase II CTD. *Genes Dev.*, **20**, 2922–2936.
32. Schreieck,A., Easter,A.D., Etzold,S., Wiederhold,K., Lidschreiber,M., Cramer,P. and Passmore,L.A. (2014) RNA polymerase II termination involves C-terminal-domain tyrosine dephosphorylation by CPF subunit Glc7. *Nat. Struct. Mol. Biol.*, **21**, 175–179.
33. Jeronimo,C., Bataille,A.R. and Robert,F. (2013) The writers, readers, and functions of the RNA polymerase II C-terminal domain code. *Chem. Rev.*, **113**, 8491–8522.
34. Qiu,H., Hu,C. and Hinnebusch,A.G. (2009) Phosphorylation of the Pol II CTD by KIN28 enhances BUR1/BUR2 recruitment and Ser2 CTD phosphorylation near promoters. *Mol. Cell*, **33**, 752–762.
35. Ahn,S.H., Kim,M. and Buratowski,S. (2004) Phosphorylation of serine 2 within the RNA polymerase II C-terminal domain couples transcription and 3′ end processing. *Mol. Cell*, **13**, 67–76.
36. Cho,E.J., Kobor,M.S., Kim,M., Greenblatt,J. and Buratowski,S. (2001) Opposing effects of Ctk1 kinase and Fcp1 phosphatase at Ser 2 of the RNA polymerase II C-terminal domain. *Genes Dev.*, **15**, 3319–3329.
37. Bermejo,R., Capra,T., Gonzalez-Huici,V., Fachinetti,D., Cocito,A., Natoli,G., Katou,Y., Mori,H., Kurokawa,K., Shirahige,K. and Foiani,M. (2009) Genome-organizing factors Top2 and Hmo1 prevent chromosome fragility at sites of S phase transcription. *Cell*, **138**, 870–884.
38. Gietz,R.D. and Sugino,A. (1988) New yeast-*Escherichia coli* shuttle vectors constructed with in vitro mutagenized yeast genes lacking six-base pair restriction sites. *Gene*, **74**, 527–534.
39. Rose,M.D., Novick,P., Thomas,J.H., Botstein,D. and Fink,G.R. (1987) A *Saccharomyces cerevisiae* genomic plasmid bank based on a centromere-containing shuttle vector. *Gene*, **60**, 237–243.
40. Holstein,E.M., Clark,K.R. and Lydall,D. (2014) Interplay between nonsense-mediated mRNA decay and DNA damage response pathways reveals that Stn1 and Ten1 are the key CST telomere-cap components. *Cell Rep.*, **7**, 1259–1269.
41. Oza,P., Jaspersen,S.L., Miele,A., Dekker,J. and Peterson,C.L. (2009) Mechanisms that regulate localization of a DNA double-strand break to the nuclear periphery. *Genes Dev.*, **23**, 912–927.
42. Fields,S. and Song,O. (1989) A novel genetic system to detect protein-protein interactions. *Nature*, **340**, 245–246.
43. Durfee,T., Becherer,K., Chen,P.L., Yeh,S.H., Yang,Y., Kilbum,A.E., Lee,W.H. and Elledge,S.J. (1993) The retinoblastoma protein associates with the protein phosphatase type I catalytic subunit. *Genes Dev.*, **7**, 555–569.
44. Garavís,M., González-Polo,N., Allepuz-Fuster,P., Louro,J.A., Fernández-Tornero,C. and Calvo,O. (2017) Sub1 contacts the RNA polymerase II stalk to modulate mRNA synthesis. *Nucleic Acids Res.*, **45**, 2458–2471.
45. Bolger,A.M., Lohse,M. and Usadel,B. (2014) Trimmomatic: a flexible trimmer for Illumina sequence data. *Bioinformatics*, **30**, 2114–2120.
46. Kim,D., Pertea,G., Trapnell,C., Pimentel,H., Kelley,R. and Salzberg,S.L. (2013) TopHat2: accurate alignment of transcriptomes in the presence of insertions, deletions and gene fusions. *Genome Biol.*, **14**, R36.
47. Ramírez,F., Ryan,D.P., Grüning,B., Bhardwaj,V., Kilpert,F., Richter,A.S., Heyne,S., Dündar,F. and Manke,T. (2016) deepTools2: a next generation web server for deep-sequencing data analysis. *Nucleic Acids Res.*, **44**, W160–W165.
48. Liao,Y., Smyth,G.K. and Shi,W. (2014) featureCounts: an efficient general purpose program for assigning sequence reads to genomic features. *Bioinformatics*, **30**, 923–930.
49. Eden,E., Navon,R., Steinfeld,I., Lipson,D. and Yakhini,Z. (2009) GOrilla: a tool for discovery and visualization of enriched GO terms in ranked gene lists. *BMC Bioinformatics*, **10**, 48.
50. García,A., Collin,A. and Calvo,O. (2012) Sub1 associates with Spt5 and influences RNA polymerase II transcription elongation rate. *Mol. Biol. Cell*, **23**, 4297–4312.
51. Allepuz-Fuster,P., Martínez-Fernández,V., Garrido-Godino,A.I., Alonso-Aguado,S., Hanes,S.D., Navarro,F. and Calvo,O. (2014). Rpb4/7 facilitates RNA polymerase CTD dephosphorylation. *Nucleic Acids Res.*, **42**, 13674–13688.
52. Langmead,B. and Salzberg,S.L. (2012) Fast gapped-read alignment with Bowtie 2. *Nat. Methods*, **9**, 357–359.
53. Li,H., Handsaker,B., Wysoker,A., Fennell,T., Ruan,J., Homer,N., Marth,G., Abecasis,G., Durbin,R. and 1000 Genome Project Data Processing Subgroup. (2009) The Sequence alignment/map (SAM) format and SAMtools. *Bioinformatics*, **25**, 2078–2079.
54. Shen,L., Shao,N., Liu,X. and Nestler,E. (2014) Ngsplot: quick mining and visualization of next-generation sequencing data by integrating genomic databases. *BMC Genomics*, **15**, 284.
55. Reja,R., Vinayachandran,V., Ghosh,S. and Pugh,B.F. (2015) Molecular mechanisms of ribosomal protein gene coregulation. *Genes Dev.*, **29**, 1942–1954.
56. Yao,S. and Prelich,G. (2002) Activation of the Bur1-Bur2 cyclin-dependent kinase complex by Cak1. *Mol. Cell Biol.*, **22**, 6750–6758.
57. Keogh,M.C., Polodny,V. and Buratowski,S. (2003) Bur1 kinase is required for efficient transcription elongation by RNA polymerase II. *Mol. Cell Biol.*, **23**, 7005–7018.
58. Espinoza,F.H., Farrell,A., Nourse,J.L., Chamberlin,H.M., Gileadi,O. and Morgan,D.O. (1998) Cak1 is required for Kin28 phosphorylation and activation in vivo. *Mol. Cell Biol.*, **18**, 6365–6373.

59. Grandin,N. and Charbonneau,M. (2001) Hsp90 levels affect telomere length in yeast. *Mol. Genet. Genomics*, **265**, 126–134.
60. Evans,S.K. and Lundblad,V. (1999) Est1 and Cdc13 as comediators of telomerase access. *Science*, **286**, 117–120.
61. Grandin,N., Damon,C. and Charbonneau,M. (2000) Cdc13 cooperates with the yeast Ku proteins and Stn1 to regulate telomerase recruitment. *Mol. Cell Biol.*, **20**, 8397–8408.
62. Shaw,R.J., Wilson,J.L., Smith,K.T. and Reines,D. (2001) Regulation of an IMP dehydrogenase gene and its overexpression in drug-sensitive transcription elongation mutants of yeast. *J. Biol. Chem.*, **276**, 32905–32916.
63. Braberg,H., Jin,H., Moehle,E.A., Chan,Y.A., Wang,S., Shales,M., Benschop,J.J., Morris,J.H., Qiu,C., Hu,F. *et al.* (2013) From structure to systems: high-resolution, quantitative genetic analysis of RNA polymerase II. *Cell*, **154**, 775–788.
64. Prelich,G. and Winston,F. (1993) Mutations that suppress the deletion of an upstream activating sequence in yeast: involvement of a protein kinase and histone H3 in repressing transcription *in vivo*. *Genetics*, **135**, 665–676.
65. Hoyos-Manchado,R., Reyes-Martín,F., Rallis,C., Gamero-Estévez,E., Rodríguez-Gómez,P., Quintero-Blanco,J., Bähler,J., Jiménez,J. and Tallada,V.A. (2017) RNA metabolism is the primary target of formamide in vivo. *Sci. Rep.*, **7**, 15895.
66. Quan,T.K. and Hartzog,G.A. (2010) Histone H3K4 and K36 methylation, Chd1 and Rpd3S oppose the functions of Saccharomyces cerevisiae Spt4-Spt5 in transcription. *Genetics*, **184**, 321–334.
67. Gasch,A.P., Spellman,P.T., Kao,C.M., Carmel-Harel,O., Eisen,M.B., Storz,G., Botstein,D. and Brown,P.O. (2000) Genomic expression programs in the response of yeast cells to environmental changes. *Mol. Biol. Cell*, **11**, 4241–4257.
68. Santos,A., Wernersson,R. and Jensen,L.J. (2015) Cyclebase 3.0: a multi-organism database on cell-cycle regulation and phenotypes. *Nucleic Acids Res.*, **43**, D1140–D1144.
69. Travers,A.A. (2003) Priming the nucleosome: a role for HMGB proteins? *EMBO Rep.*, **4**, 131–136.
70. Panday,A. and Grove,A. (2017) Yeast HMO1: linker histone reinvented. *Microbiol. Mol. Biol. Rev.*, **81**, e00037-16.
71. Goulian,M., Heard,CJ and Grimm,S.L. (1990) Purification and properties of an accessory protein for DNA polymerase α/primase. *J. Biol. Chem.*, **265**, 13221–13230.
72. Casteel,D.E., Zhuang,S., Zeng,Y., Perrino,F.W., Boss,G.R., Goulian,M. and Pilz,R.B. (2009) A DNA polymerase α/primase cofactor with homology to replication protein A-32 regulates DNA replication in mammalian cells. *J. Biol. Chem.*, **284**, 5807–5818.
73. Qi,H. and Zakian,V.A. (2000) The *Saccharomyces* telomere-binding protein Cdc13p interacts with both the catalytic subunit of DNA polymerase α and the telomerase-associated Est1 protein. *Genes Dev.*, **14**, 1777–1788.
74. Crabbé,L., Thomas,A., Pantesco,V., De Vos,J., Pasero,P. and Lengronne,A. (2010) Analysis of replication profiles reveals key role of RFC-Ctf18 in yeast replication stress response. *Nat. Struct. Mol. Biol.*, **17**, 1391–1397.
75. Mason,P.B. and Struhl,K. (2005) Distinction and relationship between elongation rate and processivity of RNA polymerase II in vivo. *Mol. Cell*, **17**, 831–840.
76. Alzu,A., Bermejo,R., Begnis,M., Lucca,C., Piccini,D., Carotenuto,W., Saponaro,M., Brambati,A., Cocito,A., Foiani,M. and Liberi,G. (2012) Senataxin associates with replication forks to protect fork integrity across RNA-polymerase-II-transcribed genes. *Cell*, **151**, 835–846.
77. Wellinger,R.J., Wolf,A.J. and Zakian,V.A. (1993) *Saccharomyces* telomeres acquire single-strand TG1–3 tails late in S phase. *Cell*, **72**, 51–60.
78. Mas,G., de Nadal,E., Dechant,R., Rodriguez de la Concepcion,M.L., Logie,C., Jimeno-Gonzalez,S., Chavez,S., Ammerer,G. and Posas,F. (2009) Recruitment of a chromatin remodelling complex by the Hog1 MAP kinase to stress genes. *EMBO J.*, **28**, 326–336.
79. Nadal-Ribelles,M., Conde,N., Flores,O., Gonzalez-Vallinas,J., Eyras,E., Orozco,M., de Nadal,E. and Posas,F. (2012) Hog1 bypasses stress-mediated down-regulation of transcription by RNA polymerase II redistribution and chromatin remodeling. *Genome Biol.*, **13**, R106.
80. Martinez,P., Thanasoula,M., Carlos,A.R., Gómez-López,G., Tejera,A.M., Schoeftner,S., Dominguez,O., Pisano,D.G., Tarsounas,M. and Blasco,M.A. (2010) Mammalian Rap1 controls telomere function and gene expression through binding to telomeric and extratelomeric sites. *Nat. Cell Biol.*, **12**, 768–780.
81. Yang,D., Xiong,Y., Kim,H., He,Q., Li,Y., Chen,R. and Songyang,Z. (2011) Human telomeric proteins occupy selective interstitial sites. *Cell Res.*, **21**, 1013–1027.
82. Ye,J., Renault,V.M., Jamet,K. and Gilson,E. (2014) Transcriptional outcome of telomere signalling. *Nat. Rev. Genet.*, **15**, 491–503.
83. Buchman,A.R., Lue,N.F. and Kornberg,R.D. (1988) Connections between transcriptional activators, silencers, and telomeres as revealed by functional analysis of a yeast DNA-binding protein. *Mol. Cell Biol.*, **8**, 5086–5099.
84. Platt,J.M., Ryvkin,P., Wanat,J.J., Donahue,G., Ricketts,M.D., Barrett,S.P., Waters,H.J., Song,S., Chavez,A., Abdallah,K.O. *et al.* (2013) Rap1 relocalization contributes to the chromatin-mediated gene expression profile and pace of cell senescence. *Genes Dev.*, **27**, 1406–1420.
85. Ungar,L., Yosef,N., Sela,Y., Sharan,R., Ruppin,E. and Kupiec,M. (2009) A genome-wide screen for essential yeast genes that affect telomere length maintenance. *Nucleic Acids Res.*, **37**, 3840–3849.